Physics – Uspekhi **54** (10) 1061 – 1084 (2011)

CONFERENCES AND SYMPOSIA

PACS numbers: 01.10.Fv, **04.20. – q**, **11.27. + d**, 89.60.Gg, 96.30.Cw, 96.30.Ys, 97.60.Jd, 97.60.Lf, **97.80. – d**, **97.82. – j**, 98.62.Sb, 98.80.Es

Astrophysics and astronomy
(Scientific session of the Physical Sciences Division of the Russian Academy of Sciences, 26 January 2011)

DOI: 10.3367/UFNe.0181.201110c.1097

An Astrophysics and Astronomy scientific session of the Physical Sciences Division of the Russian Academy of Sciences (RAS) was held in the Conference Hall of the P N Lebedev Physical Institute, RAS, on 26 January 2011.

The following reports were put on the session's agenda posted on the web site www.gpad.ac.ru of the Physical Sciences Division, RAS:

(1) **Cherepashchuk A M** (Sternberg Astronomical Institute, Moscow State University, Moscow) "Investigation of X-ray sources";

(2) **Shustov B M** (Institute of Astronomy, Russian Academy of Sciences, Moscow) "Asteroid and comet hazards: physical and other aspects";

(3) **Sazhin M V** (Sternberg Astronomical Institute, Moscow State University, Moscow) "Search for cosmic strings";

(4) **Zakharov A F** (Russian Federation State Scientific Center 'A I Alikhanov Institute for Theoretical and Experimental Physics', Moscow) "Exoplanet search using gravitational microlensing".

Papers written on the basis of the reports are published below.

PACS numbers: 97.60.Jd, 97.60.Lf, **97.80. – d**
DOI: 10.3367/UFNe.0181.201110d.1097

Optical investigations of X-ray binary systems

A M Cherepashchuk

1. Introduction

Observations in the optical range of the spectrum are critically important in the investigation of X-ray binary systems. X-ray binary systems contain relativistic objects (neutron stars and black holes) which accrete a substance of a satellite — a normal star. Optical investigations permit studying the motion of 'probe bodies' (stars, gas disks, etc.) in the gravitational field of a relativistic object, and thereby make it possible to measure the masses of neutron stars (NSs) and black holes (BHs). Mass is the most important parameter determining whether the relativistic object belongs to either the class of NSs or the class of BHs.

According to modern notions [1], with general relativity (GR) effects taken into account, when the core mass of a star which underwent chemical evolution due to thermonuclear reactions exceeds a value of $3M_{\odot}$, it eventually evolves into a BH; when the mass of the stellar core is less than $3M_{\odot}$, the stellar evolution results in the formation of a white dwarf or a neutron star. The possibility of measuring the masses of relativistic objects makes X-ray binary systems a powerful tool in the quest for BH stellar masses.

This year will observe the 40th anniversary of the launch of American dedicated X-ray satellite Uhuru into a circumterrestrial orbit, which opened up the era of systematic sky observations in the X-ray region and marked the beginning of observational BH research. In this paper, we describe the results of the 40-year-long quest for and investigations of BHs in X-ray binary systems by means of optical astronomy techniques. It should be noted that it is quite sufficient to apply Newton's law of gravitation when determining BH masses by optical techniques, because the dimensions of the orbits of X-ray binary systems are far greater than the BH gravitational (Schwarzschild) radius $r_{\rm g} = 2GM/c^2$; for a BH of mass $M = 10M_{\odot}$, this radius is equal to 30 km.

We emphasize that, since the masses of BHs in X-ray binary systems are determined using Newton's theory of gravitation, BH masses evaluated in this way are independent of the type of the relativistic theory of gravitation, because all of these theories, including those that are alternatives to GR, cross over to Newton's theory at the distance from the gravitating center.

2. Possibility of observation of black holes

According to modern concepts [1–3], a BH comprises a spacetime domain wherein the gravitational field is so strong that no signal from this domain, not even light, can escape it and turn to spatial infinity. The physical boundary of a BH is the horizon of events at which, from the viewpoint of a distant

A M Cherepashchuk Sternberg Astronomical Institute, Moscow State University, Moscow, Russian Federation
E-mail: cherepashchuk@gmail.com

Uspekhi Fizicheskikh Nauk **181** (10) 1097 – 1122 (2011)
DOI: 10.3367/UFNr.0181.201110c.1097
Translated by E N Ragozin, E G Strel'chenko, K A Postnov; edited by A Radzig

Uspekhi Fizicheskikh Nauk **181** (10) 1097 – 1104 (2011)
DOI: 10.3367/UFNr.0181.201110d.1097
Translated by E N Ragozin; edited by A Radzig

observer, the running of time comes to a halt. For a nonrotating BH, the event horizon radius r_h is equal to the gravitational (Schwarzschild) radius $r_g = 2GM/c^2$. For a rotating BH, the event horizon is submerged in the ergosphere with a vortex gravitational field and the horizon radius $r_h < r_g$.

The possibility of BH observation was first pointed out by Zel'dovich [4] and Salpeter [5] in 1964. As they noted, great energy, on the order of 10% of the rest energy of the substance, may be liberated in the nonspherical accretion of a substance on a BH. The theory of the disk accretion of a substance onto relativistic objects was elaborated in Refs [6–8].

More than one hundred compact X-ray sources, in most cases X-ray binary systems consisting of an optical star — the substance donor — and a relativistic object residing in accretion mode, were discovered from aboard the Uhuru satellite [9]. To date, several thousand X-ray binary systems have been discovered in our and other galaxies with the aid of new-generation X-ray space observatories.

The theory of disk accretion [6–8] made it possible to promptly explain the nature of the majority of the newly discovered compact X-ray sources as accreting NSs and BHs in binary systems. At the same time, this brought up the burning problem of optical identification of X-ray binary systems and of studying their optical manifestations.

The first identification of the Her X-1 X-ray binary system with the variable optical star HZ Her and the explanation of its optical variability by the 'reflection' effect, more precisely by the X-ray heating of the optical star, was made in Refs [10–12]. Lyutyi et al. [13] discovered the optical variability of the Cyg X-1 X-ray binary system — 'the No. 1 candidate' for a black hole — and interpreted this variability as the ellipsoidality effect of the optical star. Webster and Murdin [14] measured the mass function of the optical star in the Cyg X-1 system, which was indicative of the presence of a BH in this system. The authors of Ref. [13] proposed a method of estimating the orbit inclination i for an X-ray binary system from the observed 'ellipsoidal' variability of an optical star, and made one of the first BH mass estimates on this basis: $m_x > 5.6M_\odot$.

The reflection and ellipsoidality effects turned out to be typical observational manifestations of X-ray binary systems in the visible and near-infrared spectral regions. These effects are widely used for optical identification of X-ray binary systems: coincidence of the periods and phases of optical and X-ray variabilities proves the reliability of identification. Furthermore, the reflection and ellipsoidality effects are much used to estimate the orbit inclinations of X-ray binary systems and determine the masses of relativistic objects (see, for instance, review Refs [15, 16]). The author of Ref. [17] discovered optical eclipses in a unique object, SS 433, with collimated precessing relativistic ejections — jets [18]. This was proof that the SS 433 object comprises a massive X-ray binary system residing at an advanced stage of evolution, which contains an optically bright, supercritical accretion disk around a relativistic object [6], the disk precessing with a period of ~ 162 days. The SS 433 object turned out to be the first representative of the objects of a new class — microquasars; the number of such objects discovered in the Galaxy ranges up to about twenty to date. The study of microquasars sheds light on the nature of quasars and galactic nuclei, in which relativistic jets are also frequently observed, though on scales several million times greater than in microquasars.

3. Methods for determining the masses of black holes in X-ray binary systems

X-ray and optical investigations of X-ray binary systems complement each other nicely. X-ray observations from dedicated satellites permit judging the presence of a compact object in a binary system and estimating — from the fast variability of X-ray emission in a time Δt, down to 10^{-3} s — its characteristic dimensions: $r \leqslant c\Delta t \leqslant 300$ km. Optical (spectral and photometric) ground-based observations provide the possibility of investigating the motion of the optical star and thereby a way of estimating the mass of the compact object. If its measured mass is greater than $3M_\odot$, it may be regarded as a candidate for a BH.

The world of X-ray binary systems is quite rich and diverse in its characteristics and observational manifestations (see *Catalogue* [19]). Here, we enlarge on only one aspect of the problem of X-ray binary systems, involving mass determination for stellar BHs (see, for instance, review [15]).

Doppler lineshifts in the spectrum of a binary system are employed to construct the curve of ray velocities of an optical star, and its mass function is determined in the model of a system containing two point masses in Keplerian orbits:

$$f_v(M) = \frac{M_x^3 \sin^3 i}{(M_x + M_v)^2} = 1.038 \times 10^{-7} K_v^3 P (1 - e^2)^{3/2}, \quad (1)$$

where M_x and M_v are the masses of the relativistic object and the optical star (in solar masses), K_v is the observed half-amplitude of the ray velocity curve of the optical star (in km s^{-1}), P is the orbital period of the system (in days), and e is the eccentricity of the orbit (determined from the departure of the ray velocity curve from a sinusoid). The mass function $f_v(M)$ is an observable quantity and has the dimensionality of mass. It constitutes the lower bound on the mass of the relativistic object. For instance, for the Cyg X-1 system, $f_v(M) \simeq 0.24M_\odot$, and for the GRS $1915+105$ system, $f_v(M) \simeq 9.5M_\odot$ (see review [15]). In the latter case, it can be said with confidence that the GRS $1915+105$ system contains a BH with a mass greater than $9.5M_\odot$.

From Eqn (1) follows an expression for the mass of a BH:

$$M_x = f_v(M)\left(1 + \frac{1}{q}\right)^2 \frac{1}{\sin^3 i}, \quad (2)$$

where $q = M_x/M_v$ is the BH-to-optical star mass ratio. Therefore, despite the fact that the X-ray binary system components are not seen separately, by using formula (2) and the values of parameters q, i determined from additional data, it is possible to evaluate the BH mass.

As noted above, orbit inclination i is determined by analyzing the optical light curve of an X-ray binary system caused primarily by the ellipsoidality effect of the optical star [13]. This method, which was proposed for X-ray binary systems in Ref. [13], is currently the only reliable method for estimating parameter i in the case where there are no X-ray eclipses in the system.

The mass ratio q is estimated from the rotational line broadening in the spectrum of the optical star: for a fixed angular velocity of orbiting, the linear velocity of stellar rotation at the equator increases with stellar radius; in X-ray binary systems, this radius is close to that of the critical Roche cavity of the optical star. Since this radius depends on the mass ratio q, we obtain the following formula for estimating

the q parameter:

$$v_{\rm rot} \sin i = 0.462\, K_{\rm v}\, \frac{1}{q^{1/3}} \left(1+\frac{1}{q}\right)^{2/3}, \qquad (3)$$

where $v_{\rm rot}$ is the equatorial velocity of stellar rotation (the value of $v_{\rm rot} \sin i$ is determined from the line profile observed).

Therefore, the use of formulas (1)–(3) in the simplest model of two point masses enables determining the mass of the BH in a binary system. Modern methods of determining the masses of BHs in X-ray binary systems are given at greater length in review [15].

When the mass ratio $q \gg 1$, a material point model may be applied to the optical star as a satisfactory approximation, because the Roche cavity dimensions for the star are relatively small. However, at $q \approx 1$, and even more so for $q < 1$, the application of the material point model to the optical star in an X-ray binary system is not quite correct, because for $q < 1$ the center of mass of the binary system lies within the bulk of the optical star. The parts of the optical star located on different sides of the center of mass of the binary system move in different directions in their orbital motion, resulting in a strong distortion of the line profile in the stellar spectrum and, accordingly, in a distortion of the ray velocity curve. That is why taking into account the real figure of the optical star in the analysis of ray velocity curves for X-ray binary systems is critical for the correct determination of the masses of relativistic objects.

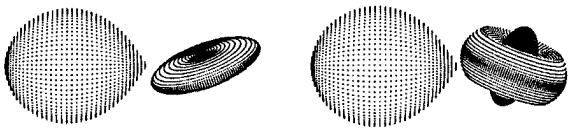

Figure 1. Mathematical models of an X-ray binary system with an accretion disk precessing around the relativistic object.

In our group, we have developed methods for interpreting the light curves, spectral line profiles, and ray velocity curves of X-ray binary systems with the inclusion of the tidal-rotational deformation of the optical star and its heating by the X-ray radiation of the accreting relativistic object, as well as with the inclusion of the presence of an accretion disk around the object [20–22] (Fig. 1). In the calculation of local line profiles in the spectrum of the optical star, advantage is taken of the methods and results of analysis of the spectra of stellar atmospheres developed by N A Sakhibullin [23]. The stellar surface is divided into several thousand elementary areas. By way of solution of the radiation transfer equation with nonzero external boundary conditions, the intensity of radiation emanating from every surface area in the direction of a terrestrial observer is calculated as a function of wavelength; included next are the Doppler shifts of the local line profiles and the mutual eclipses of the components. Summing up the contributions from all surface areas seen by the observer permits calculating the theoretical light curve for a star with a complex shape, the integral profiles of absorption lines in its spectrum, and, accordingly, the theoretical ray velocity curve (Fig. 2). Since the optical star in an X-ray binary system has a pear-like shape with a complex temperature distribution over the surface, the line profiles in its spectrum vary appreciably with the phase of the orbital period, resulting in the consequential distortion of the ray velocity curve in comparison with that in the model of two point masses. It is precisely this distorted theoretical ray velocity curve that should be compared with the observational data in the determination of the BH mass in an X-ray binary system (see Fig. 2).

The application of the more realistic X-ray binary system model and modern statistical criteria for substantiating the adequacy of the model to observed data [24] makes it possible

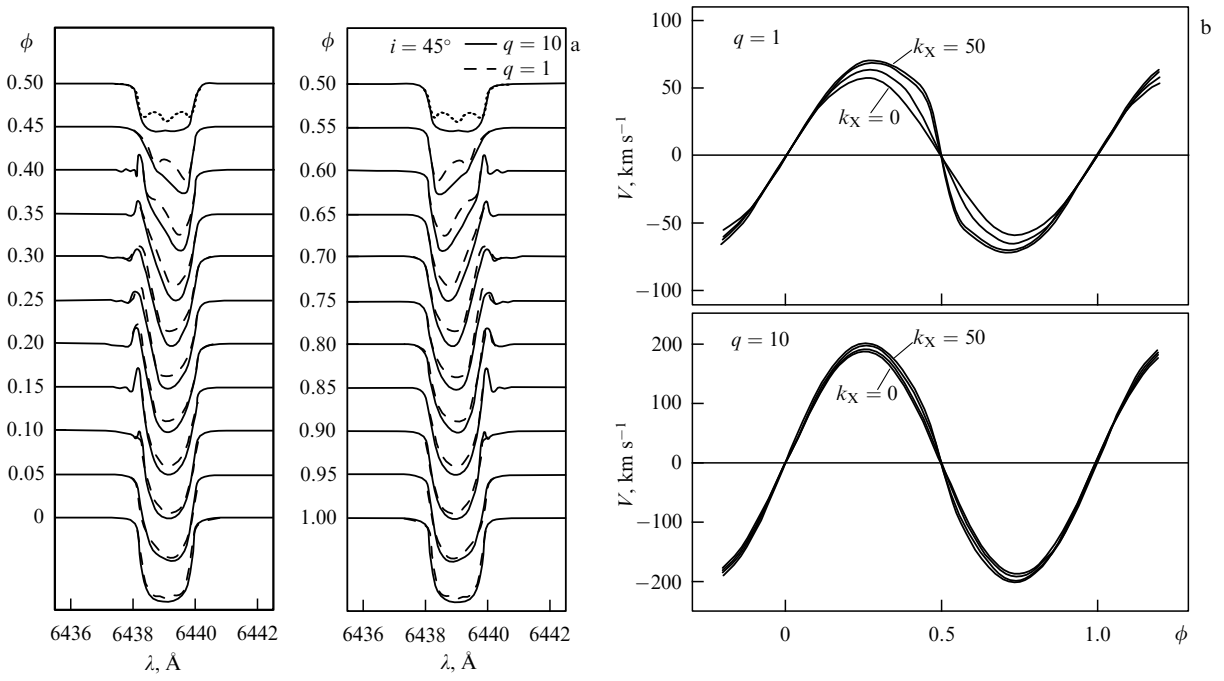

Figure 2. (a) Variation of the CaI absorption line profile in the optical spectrum of an X-ray binary system associated with a variation of optical period phase ϕ, which arises from the tidal deformation of the star and the heating of its surface by X-ray radiation of the accreting relativistic object. For the sake of convenience in comparing the profiles, Doppler line shifts caused by orbital motion are eliminated. (b) Appropriate ray velocity curves for different values of component mass ratio q and X-ray heating parameter k_X. The orbit of the system is circular.

to obtain the most reliable parameter values and their confidence intervals (errors).

Let us give several examples of the efficient use of our methods. We showed in Ref. [25] that the masses of X-ray pulsars in binaries with OB supergiant satellites, determined in the framework of the simplest model of the system as a system of two point masses, are underrated by 5–10%. This result is important for improving the equation of state of a neutron substance.

From the analysis of the high-precision ray velocity curve of the Cyg X-1 X-ray binary system, which encompassed the observational data over 502 nights, we were able to estimate the orbit inclination of the system: $i < 45°$, and provide an independent estimate of the BH mass: $M_x = (8.5-13.6)\,M_\odot$ [26].

The inclusion of strong X-ray heating of the optical star in the 2S0921-63 X-ray binary system led to a substantial lowering of the relativistic object mass, and this object was shown to be an NS rather than a low-mass BH [27].

It is pertinent to note that the profiles of absorption lines in the optical spectra of X-ray binary systems are calculated in our model both under the assumption of local thermodynamic equilibrium and neglecting this hypothesis, when a system of equations for the stationary populations of several hundred atomic and ionic energy levels is solved to construct the corresponding source functions.

4. Masses of black holes in X-ray binary systems

During the past four decades, owing to the vigorous investigations carried out by teams of Russian and foreign researchers in both the X-ray and optical spectral regions, it has been possible to accumulate valuable data about the masses of a wealth of BHs and NSs. A new realm of astrophysics has come into existence — the demography of BHs — which studies the origin and growth of BHs, and the association of these extreme objects with other objects in the Universe: stars, galaxies, etc. (see, for instance, review [15]).

The masses of 24 stellar BHs and the masses of about 50 NSs have been measured in binary systems to date (Fig. 3).

The masses of NSs lie in the (1–2) $M_\odot$ range, the average NS mass being $\sim 1.4M_\odot$. All of these 50 objects exhibit clear evidences of an observable surface: radio pulsars, X-ray pulsars, or type-I X-ray bursters. Recall that the phenomenon of a radio pulsar is associated with the fast axial rotation of an NS (with a period between 1 and 10^{-3} s) and the strong magnetic field ($\sim 10^{12}$ G) of the NS 'attached' to its surface. The phenomenon of an X-ray pulsar reflects the presence of hot X-ray regions (shock waves) near the magnetic poles of a fast-rotating strongly magnetized NS, while the type-I X-ray burster phenomenon is due to thermonuclear explosions of the substance accumulated in the course of accretion on the surface of an NS with a weak magnetic field. The X-ray pulsar, type-I X-ray burster, and radio pulsar phenomena would be impossible if the NSs did not possess observable surfaces. We emphasize that the fast axial rotation and the strong magnetic field are the natural consequences of compression of the stellar nucleus to the very small size ($\sim$ 10 km) of a compact relativistic object at the end of evolution.

Therefore, whenever a compact object shows evidences of an observable surface (a radio pulsar, X-ray pulsar, or type-I X-ray burster phenomenon), its measured mass does not exceed $3M_\odot$, which is in perfect agreement with the predictions of GR (!). We are reminded that the number of measured masses is quite high in this case, amounting to fifty.

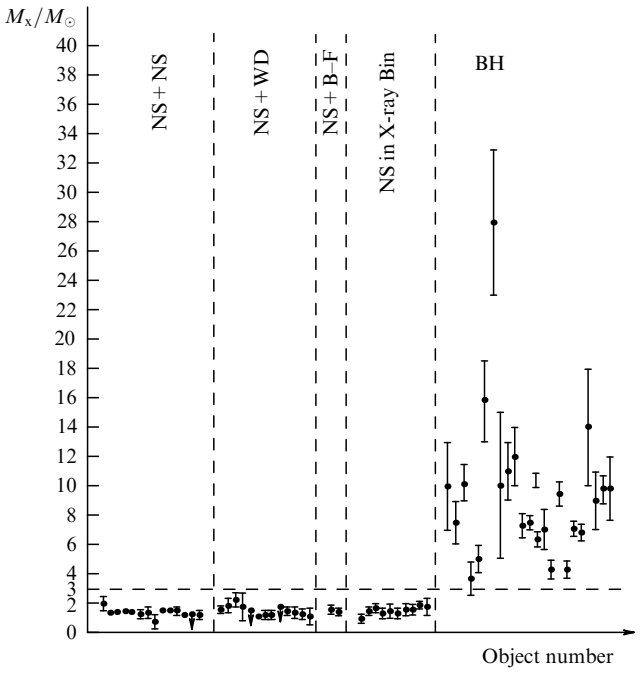

Figure 3. Measured masses of neutron stars (NSs) and black holes (BHs) in binary systems: NS + NS — a radio pulsar in combination with a neutron star; NS + WD — a radio pulsar in combination with a white dwarf; NS + B-F — a radio pulsar in combination with a nondegenerate star of the B-F spectral class, and NS in X-ray Bin — an X-ray pulsar in a binary system. The dashed horizontal line intercepts a mass value of $3M_\odot$ — the absolute upper bound on the mass of a neutron star predicted by GR.

The masses of 24 BHs lie in the (4–25) $M_\odot$ range. The average BH mass equals $\sim 9M_\odot$. According to the predictions of GR, a BH should not possess an observable surface, but only an event horizon — a light surface in spacetime. That is why, according to GR, a BH should not exhibit the properties of a radio pulsar, an X-ray pulsar, or a type-I X-ray burster (type II bursters, which are associated with instabilities developing in the inner parts of the accretion disk, may be observed — they are easily distinguished from type I bursters). Such is indeed the case with the 24 BHs studied: none of these massive ($M > 3M_\odot$) compact objects is a radio pulsar, an X-ray pulsar, or a type-I X-ray burster (!). These massive ($M > 3M_\odot$) compact objects — candidates for a BH — exhibit only an irregular or quasiperiodic (but not strictly periodic) variability of X-ray emission over time periods from ~ 0.1 to ~ 0.001 s, which permits estimating the characteristic dimensions of these objects, as discussed in the foregoing. In the model of oscillations of the inner parts of an accretion disk or the orbital motion of hot spots, it is possible to show that so fast an X-ray variability of the known candidates for BHs is due to their very small dimensions which do not exceed several gravitational radii r_g.

Therefore, as data on the masses of relativistic objects accumulate, the following result is taking shape: NSs and BHs differ not only by mass, but also by their observational manifestations, in perfect quantitative agreement with GR; a discontinuity in the observational manifestations of relativistic objects makes itself evident in the vicinity of the theoretically predicted mass value of $3M_\odot$ (the upper bound

on the mass of an NS). Objects having masses greater than $3M_\odot$ (i.e., BHs) exhibit no clear signs of an observable surface; meanwhile, when a compact object shows clear indications of an observable surface, its measured mass does not exceed $3M_\odot$.

However, we would do well to bear in mind that some NSs may not show manifestations of an observable surface. For instance, a radio pulsar or an X-ray pulsar phenomenon may not be observed owing to the 'unfortunate' orientation of the magnetic dipole axis relative to the observer or when the NS rotation axis coincides with the axis of the magnetic dipole. That is why the distinctions between the vivid observable manifestations of NSs and BHs noted above are only the necessary, but not the sufficient, criterion that the 24 investigated candidates for BHs are real BHs. Nevertheless, the large number of objects studied (24) gives us confidence that the BHs of stellar masses do exist. This confidence will strengthen with the accumulation of new observational data about the masses of relativistic objects in binary systems. Recently, in connection with the putting into operation of new large 8–10-meter optical telescopes, the possibility has opened up of studying X-ray binary systems in other galaxies, which may lead to a substantial increase in the number of NSs and BHs with measured masses.

In addition to the clear distinctions between the observational manifestations of NSs and BHs described in the foregoing, there are also subtle distinctions between them, which are related to the shape of their X-ray spectra and the character of their X-ray emission intensity variation in time (see, for instance, Ref. [15]). These subtle distinctions also testify that NSs, unlike BHs, possess observable surfaces.

5. Demography of stellar black holes

We describe several findings of the demographic investigations of BH stellar masses.

It turns out that there is no dependence between the mass of a relativistic object and the mass of its satellite in binary systems: both NSs and BHs are found in binary systems, with satellites having both a large mass and a small mass. There is no BH–satellite mass dependence in a binary system, either. In this sense, close binary systems with NSs and BHs are similar to classical close binary systems, in which arbitrary component combinations are found, as repeatedly emphasized by D Ya Martynov [28].

Some interesting features of the mass distribution of NSs and BHs were also brought to light [29, 30]. First, the number of investigated stellar BHs does not increase with decreasing BH mass (Fig. 4). This comes as a surprise, because the stellar mass distribution in the Galaxy is such that the number of stars rises steeply (as M^{-5}) with decreasing stellar mass. Since stellar BHs are formed in the collapses of the iron nuclei of massive stars ($M > 30M_\odot$), one would think that the number of stellar BHs should rise sharply towards smaller masses, but this is not observed. It may be shown [15] that this extraordinary fact is not related to observational selection effects. Second, a dip begins to show itself in the mass distribution of NSs and BHs in the mass range from $2M_\odot$ to $4M_\odot$. In this mass interval, the number of discovered NSs and BHs is close to zero, which is also unlikely to arise from the observational selection effects [15]. If the inference about the presence of a dip in the mass distribution of NSs and BHs in the (2–4) $M_\odot$ interval is confirmed by future observations, it will call for a serious theoretical interpretation.

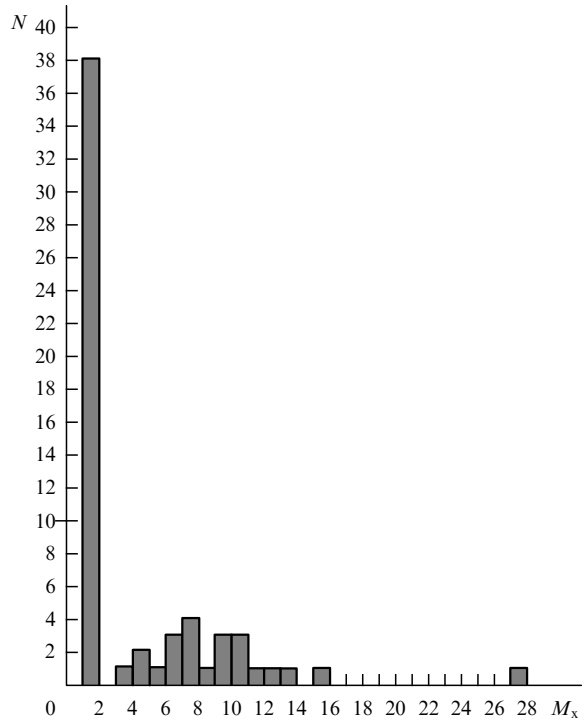

Figure 4. Histogram of the mass distribution of neutron stars and black holes in binary systems. The high peak at the left of the drawing corresponds to neutron stars.

In this connection, mention should be made of an interesting opportunity to explain the unusual stellar BH mass distribution. The authors of Ref. [31] came up with the idea that the flat mass distribution of stellar BHs and the dip in this distribution in the (2–4) $M_\odot$ interval may be due to enhanced quantum evaporation of BHs, which follows from several multidimensional gravitation models (see, for instance, Ref. [32]). In these gravitation models, the time τ for the quantum evaporation of a BH is much shorter than the Hawking time [33], and may be estimated by the formula

$$\tau \sim 1.2 \times 10^2 \left(\frac{M}{M_\odot}\right)^3 \left(\frac{1\ \text{mm}}{L}\right)^3, \qquad (4)$$

where M is the BH mass, and L is the characteristic scale length of the additional (fourth) spatial dimension. For an average BH mass of $\sim 9M_\odot$ and the expected upper bound on the L quantity of several hundredths of a millimeter, the quantum evaporation time reaches $\sim 10^8$ years, which is much smaller than the age of the Universe and is comparable to the period of nuclear evolution of the stars. Since the rate of quantum evaporation rises steeply with a lowering of BH mass, it is believed that the observed deficit of small-mass BHs is due to the fact that many BHs with small masses managed to evaporate during the lifetime of the Universe. It is remarkable in this model that the known value of the observed average stellar BH mass of $9M_\odot$ permits imposing a constraint on the value of the L parameter, which is consistent with the constraints following from the data of laboratory physical experiments [34].

Furthermore, if the characteristic stellar BH evaporation time is shorter than the age of the Universe ($\sim 1.4 \times 10^{10}$ years), a decrease in BH mass in an X-ray binary system should lead to an observable change in its

orbital period. The quest for such changes in the orbital periods of X-ray binary systems is currently underway (including in our group). As a result of this research, it has been possible to obtain the upper constraint on the characteristic length scale of the additional spatial dimension: $L < 0.1$ mm [35]. Further accumulation of observational data on the variation of X-ray binary system periods will permit a substantial improvement in this estimate.

There are also other, less exotic, explanations for the anomalous mass distribution of stellar BHs, which are related to the mass loss by massive stars in the form of stellar wind [29], and to the features of the late stages of massive star evolution [36, 37].

It should be emphasized that the existence of a dip in the observable relativistic object mass distribution over the (2–4) $M_\odot$ region (the supposition of its existence was made in Refs [38, 39]) was recently confirmed by a rigorous statistical analysis of the latest observational data on BH masses in X-ray binary systems [40].

Recent years have seen a constant strengthening of the viewpoint that the collapses of the carbon–oxygen nuclei of Wolf-Rayet stars with a fast axial rotation, which give rise to extremely fast rotating (Kerr) BHs in different galaxies, may be the sources of the famous and so far mysterious cosmic gamma-ray bursts whereat an enormous amount of energy is released in several seconds in the gamma-ray range, this energy being comparable to the energy liberated in the annihilation of the entire solar mass. As noted in Ref. [41], the orbital motion of a close satellite in a very close binary system maintains, owing to the tidal mechanism, the fast axial rotation of the star — the precursor of a Kerr BH — despite a substantial loss of the angular momentum of the star's rotation in throwing off its shell during the supernova explosion. Therefore, there are grounds to believe that in the observation of cosmic gamma-ray bursts we directly 'witness' the formation of stellar BHs in very close binary systems.

Two types of quasiperiodic (but not strictly periodic) oscillations (QPOs) of X-ray emission intensity are observed in X-ray binary systems with BHs: low-frequency QPOs (LFQPOs) with frequencies of $\sim 0.1-30$ Hz, and high-frequency QPOs (HFQPOs) whose frequencies lie in the 40–450 Hz range (see, for instance, Refs [42–44]). The low-frequency QPOs may be observable for several days or even months. For the GRS $1915+105$ system with a BH, for instance, QPOs with a frequency of 2.0–4.5 Hz were observed for 6 months in 1996–1997. Furthermore, this system also exhibited high-frequency QPOs with frequencies of 41 and 67 Hz, as well as with frequencies of 113 and 168 Hz.

Attempts to relate low-frequency QPOs to the geometrical and physical characteristics of accretion plasma run into difficulties, because LFQPOs correspond to frequencies which are much lower than those inherent in the orbits in the inner parts of the accretion disk. For a BH with a mass of $10\,M_\odot$, for instance, an orbital frequency of 3 Hz corresponds to a disk radius of $100r_g$, while the assumed radius of the domain of maximum energy liberation in the X-ray region lies in the $(1–10)\,r_g$ range, depending on the BH rotation parameter. Numerous LFQPO models treat this phenomenon in the framework of different oscillation mechanisms of the disk or its structures (see, for instance, Ref. [45]).

High-frequency QPOs have a direct bearing on the processes occurring near the radius of the last stable orbit around a BH, since the orbital frequency for the last stable orbit is equal to $220\ \text{Hz}\times(M/10\,M_\odot)^{-1}$ for a Schwarzschild BH, and to $1615\ \text{Hz}\times(M/10\,M_\odot)^{-1}$ for a Kerr BH [44]. Interestingly, the high-frequency QPOs emerge in pairs with frequencies at the ratio of 3:2. Examples of such systems are as follows: GRO J1655-40 (300, 450 Hz), XTE J1550-564 (184, 276 Hz), GRS $1915+105$ (113, 168 Hz), and H1743-322 (165, 241 Hz). Observed in the GRS $1915+105$ system is a second pair of high-frequency QPOs (41, 67 Hz), whose frequencies are not in the ratio of 3:2.

The ratio of 3:2 in high-frequency QPOs constitutes evidence that the HFQPOs are caused by some resonance effects in the oscillations of the inner parts of the accretion disk, which are described in the framework of GR (see, for instance, Refs [46–48]). As noted in Ref. [43], a relationship between the HFQPO frequency and the BH mass in an X-ray binary system is beginning to show up:

$$f_0 \simeq 931\left(\frac{M_{\rm BH}}{M_\odot}\right)^{-1}\ \text{Hz}\,,$$

where f_0 is the fundamental frequency of the pair of frequencies, so that the observed frequencies are $2f_0$ and f_0.

In recent years, a close similarity has been established between X-ray binary systems with BHs and galactic nuclei [49]. In particular, a statistical relationship termed the fundamental plane was discovered for supermassive and stellar BHs [50]:

$$\lg L_{\rm R} = (0.60^{+0.11}_{-0.11})\lg L_{\rm X} + (0.78^{+0.11}_{-0.09})\lg M_{\rm BH} + 7.33^{+4.05}_{-4.07}\,,$$

where $L_{\rm R}$ is the radio luminosity (caused primarily by the jet's radio emission), $L_{\rm X}$ is the X-ray luminosity (primarily due to the emission of the accretion disk), and $M_{\rm BH}$ is the mass of a BH (supermassive and stellar alike).

It was also established that the variability of active galactic nuclei is similar to the variability of accreting stellar BHs in binary systems, when this variability is normalized according to the BH mass and accretion rate [49]. It is well known that the X-ray variability of active galactic nuclei and BHs in binaries may be described by the variability power spectral density $P(\nu)$, where ν is the frequency ($1/\nu$ is the characteristic time). For long characteristic times, the $P(\nu)$ function may be approximated by a power law: $P(\nu) \sim \nu^{-\alpha}$, where $\alpha \approx 1$. This power law spectrum exhibits a break at shorter characteristic times to assume the form $P(\nu) \sim \nu^{-\alpha}$, where $\alpha \geqslant 2$. The corresponding spectrum break frequency is denoted as $\nu_{\rm B}$, and the characteristic spectrum break time as $T_{\rm B} = 1/\nu_{\rm B}$. Then, when $T_{\rm B}$ and $L_{\rm bol}$ (the luminosity which characterizes the rate of accretion) are determined from observations, the BH mass $M_{\rm BH}$ may be estimated from the relationship

$$\lg T_{\rm B} = 2.1\lg M_{\rm BH} - 0.981\lg L_{\rm bol} - 2.32\,.$$

We emphasize that this statistical relationship is true both for stellar BHs and for supermassive BHs in galactic nuclei. The black holes in binaries which are in accretion mode exhibit aperiodic variability of X-ray emission over times ranging from several days to $10^{-2}-10^{-3}$ s. Suchlike variability is also observed in the emission of supermassive BHs, though on longer time scales — from several years to several months and weeks.

Such are the main observational features of the stellar BH demography. Estimates made on the basis of the above observed data (with the inclusion of observational selection

effects) show that the total number of stellar BHs in our Galaxy should be of order 10^7. For an average BH mass of (9–10) $M_\odot$, the total mass of stellar BHs amounts to $\sim 10^8 M_\odot$, or about 0.1% of the mass of the visible baryon substance of our Galaxy contained in stars, gas, and dust. It should also be noted that the total mass of stellar BHs in the Galaxy is more than an order of magnitude (~ 25 times) greater than the mass of the supermassive BH ($4.3 \times 10^6 M_\odot$) located at the galactic center [51].

6. Conclusion

Over the past 40 years, major advances have been made towards the solution to the problem of the quest for and investigation of stellar BHs in X-ray binary systems. This progress is due to the power of ground-based optical telescopes and the unique possibilities furnished by cosmic observations in the X-ray spectral region.

Several dozen massive and extremely compact objects have been discovered, the observed properties of these objects bearing a great resemblance to the properties of BHs predicted by Albert Einstein's GR. The whole set of observational data on these numerous massive and compact objects agrees nicely with the predictions of GR. This, as V L Ginzburg himself expressed one day, strengthens our confidence in the existence of BHs in the Universe.

References

1. Zel'dovich Ya B, Novikov I D *Teoriya Tyagoteniya i Evolyutsiya Zvezd* (The Theory of Gravitation and Evolution of Stars) (Moscow: Nauka, 1971)
2. Novikov I D, Frolov V P *Fizika Chernykh Dyr* (Physics of Black Holes) (Moscow: Nauka, 1986) [Translated into English (Dordrecht: Kluwer Acad., 1989)]
3. Novikov I D, Frolov V P *Usp. Fiz. Nauk* **171** 307 (2001) [*Phys. Usp.* **44** 291 (2001)]
4. Zel'dovich Ya B *Dokl. Akad. Nauk SSSR* **155** 67 (1964) [*Sov. Phys. Dokl.* **9** 195 (1964)]
5. Salpeter E E *Astrophys. J.* **140** 796 (1964)
6. Shakura N I, Sunyaev R A *Astron. Astrophys.* **24** 337 (1973)
7. Pringle J E, Rees M J *Astron. Astrophys.* **21** 1 (1972)
8. Novikov I D, Thorne K S, in *Black Holes* (Eds C DeWitt, B S DeWitt) (New York: Gordon and Breach, 1973) p. 343
9. Giacconi R et al. *Astrophys. J.* **167** L67 (1971)
10. Kurochkin N E *Peremennye Zvezdy. Byull.* **18** 425 (1972)
11. Cherepashchuk A M et al. *Inform. Bull. Var. Stars* **720** 1 (1972)
12. Bahcall J N, Bahcall N A *Astrophys. J.* **178** L1 (1972)
13. Lyutyi V M, Syunyaev R A, Cherepashchuk A M *Astron. Zh.* **50** 3 (1973) [*Sov. Astron.* **17** 1 (1973)]
14. Webster N L, Murdin P *Nature* **235** 37 (1972)
15. Cherepashchuk A M *Usp. Fiz. Nauk* **173** 345 (2003) [*Phys. Usp.* **46** 335 (2003)]
16. Charles P A, in *Black Holes in Binaries and Galactic Nuclei: Diagnostics, Demography and Formation* (Eds L Kaper, E P J van den Heuvel, P A Woudt) (Berlin: Springer-Verlag, 2001) p. 27
17. Cherepashchuk A M *Mon. Not. R. Astron. Soc.* **194** 761 (1981)
18. Margon B *Annu. Rev. Astron. Astrophys.* **22** 507 (1984)
19. Cherepashchuk A M et al. *Highly Evolved Close Binary Stars* Vol. 1 *Catalogue* (Amsterdam: Gordon and Breach, 1996)
20. Antokhina E A, Cherepashchuk A M *Astron. Zh.* **71** 420 (1994) [*Astron. Rep.* **38** 367 (1994)]
21. Antokhina E A, Cherepashchuk A M, Shimanskii V V *Astron. Zh.* **82** 131 (2005) [*Astron. Rep.* **49** 109 (2005)]
22. Cherepashchuk A M *Astrophys. Space Sci.* **304** 263 (2006)
23. Sakhibullin N A *Metody Modelirovaniya v Astrofizike. I. Zvezdnye Atmosfery* (Simulation Methods in Astrophysics. I. Stellar Atmospheres) (Kazan: Fen, 1997)
24. Goncharskii A V, Romanov S Yu, Cherepashchuk A M *Konechnoparametricheskie Obratnye Zadachi Astrofiziki* (Finite-Parametric Inverse Problems in Astrophysics) (Moscow: Izd. MGU, 1991)
25. Abubekerov M K, Antokhina É A, Cherepashchuk A M *Astron. Zh.* **81** 108 (2004) [*Astron. Rep.* **48** 89 (2004)]
26. Abubekerov M K, Antokhina E A, Cherepashchuk A M *Astron. Zh.* **81** 606 (2004) [*Astron. Rep.* **48** 550 (2004)]
27. Abubekerov M K et al. *Astron. Zh.* **83** 602 (2006) [*Astron. Rep.* **50** 544 (2006)]
28. Martynov D Ya *Usp. Fiz. Nauk* **108** 701 (1972) [*Sov. Phys. Usp.* **15** 365 (1972)]
29. Cherepashchuk A M *Astron. Zh.* **78** 145 (2001) [*Astron. Rep.* **45** 120 (2001)]
30. Cherepashchuk A M *Usp. Fiz. Nauk* **172** 959 (2002) [*Phys. Usp.* **45** 896 (2002)]
31. Postnov K A, Cherepashchuk A M *Astron. Zh.* **80** 1075 (2003) [*Astron. Rep.* **47** 989 (2003)]
32. Randall L, Sundrum R *Phys. Rev. Lett.* **83** 4690 (1999)
33. Hawking S W *Nature* **248** 30 (1974)
34. Long J C, Price J C *C. R. Physique* **4** 337 (2003)
35. Johannsen T, Psaltis D, McClintock J E *Astrophys. J.* **691** 997 (2009)
36. Postnov K A, Prokhorov M E *Astron. Zh.* **78** 1025 (2001) [*Astron. Rep.* **45** 899 (2001)]
37. Fryer C L, Kalogera V *Astrophys. J.* **554** 548 (2001)
38. Bailyn C D et al. *Astrophys. J.* **499** 367 (1998)
39. Cherepashchuk A M, in *Sovremennye Problemy Zvezdnoi Evolyutsii. Trudy Mezhdunar. Konf. "Problemy Zvezdnoi Evolyutsii", Posvyashchennoi 80-Letiyu A.G. Masevich* (Modern Problems of Stellar Evolution. Proc. of the Intern. Conf. "Problems of Stellar Evolution" Dedicated to the 80th Anniversary of the birth of A.G. Masevich), *Zvenigorod, 13–15 October 1998* (Ed. D Z Vibe) (Moscow: GEOS, 1998) p. 198
40. Özel F et al. *Astrophys. J.* **725** 1918 (2010)
41. Tutukov A V, Cherepashchuk A M *Astron. Zh.* **81** 43 (2004) [*Astron. Rep.* **48** 39 (2004)]
42. McClintock J E, Remillard R A, astro-ph/0306213
43. Remillard R A, McClintock J E *Annu. Rev. Astron. Astrophys.* **44** 49 (2006)
44. McClintock J E, in *Short-Period Binary Stars: Observations, Analyses, and Results* (Eds E F Milone, D A Leahy, D W Hobill) (Berlin: Springer, 2008) p. 3
45. Titarchuk L, Osherovich V *Astrophys. J. Lett.* **542** L111 (2000)
46. Abramowicz M A, Kluzniak W *Astron. Astrophys.* **374** L19 (2001)
47. Török G et al. *Astron. Astrophys.* **436** 1 (2005)
48. Kato Y *Publ. Astron. Soc. Jpn.* **56** 931 (2004)
49. McHardy I M et al. *Nature* **444** 730 (2006)
50. Merloni A, Heinz S, Di Matteo T *Mon. Not. R. Astron. Soc.* **345** 1057 (2003)
51. Gillessen S et al. *Astrophys. J. Lett.* **707** L114 (2009)

PACS numbers: 89.60.Gg, 96.30.Cw, 96.30.Ys
DOI: 10.3367/UFNe.0181.201110e.1104

Asteroid and comet hazards: the role of physical sciences in solving the problem

B M Shustov

1. Introduction

Starting in the 1990s, the problem of hazardous impacts of sufficiently large celestial objects (asteroids and comets) with Earth (the asteroid–comet hazard, or ACH) attracted marked attention from scientists, technicians, politicians, the military and the general public, both globally and in Russia. Over the last decade and a half, hundreds of scientific papers and seven monographs have been published on this topic in the Russian language alone. A fairly comprehensive and up-to-date review can be found in a recent monograph [1] which, for the first time in the Russian literature, provides a thorough and detailed discussion of all aspects of the ACH problem.

An impact of a Tunguska type object (say, 50 m in size with a speed of 20 km s^{-1}) would release an energy of about 10 megatons of TNT, resulting in what can be defined as a local catastrophe. Based on the total damage area of about 2000 km^2 in the Tunguska event, an impact of Earth with a 300-m asteroid (for example, Apophis) would have a more damaging effect than would the entire global arsenal of explosives. With many tens of thousands of square kilometers of total damage area (a regional catastrophe), this impact will have severe continental-scale consequences. Space objects larger than a kilometer will produce in falling on Earth consequences of global significance.

Impacts of Earth with minor solar system bodies (dust particles, meteoroids, asteroids, and comets) are rarely dangerous. Average rate estimates for such impacts and their qualitative consequences are listed in Table 1.

Very small size objects enter Earth's atmosphere in a virtually continuous flow without noticeably affecting our lives. Nor do larger, meter-sized objects, so spectacular as they enter and break up in the atmosphere and fall on the ground, cause any serious trouble. Denoting by D the size of a body, the following scalings can be used for back-of-an-envelope purposes: the body energy $E \propto D^3$, and the collision frequency $f \propto D^{-2}$ (see Ref. [2]). The average (destruction) energy e released per unit time on the ground due to an impact with a body of size D is, to a first approximation, proportional to D. This means that over larger time intervals larger bodies carry more energy e than their smaller counterparts and hence represent a higher average degree of threat than smaller ones (see Section 3 for a discussion on average versus specific risk). On the other hand, impacts with objects more than a kilometer in size are so rare on the time scale of *homo sapiens* existence that, in spite of their deadly consequences, they are primarily a subject for experts in the geophysical and biological histories of Earth. From a practical point of view, this means that impacts with celestial objects measuring from about 30–50 m to about 0.5–1.0 km should be given the most attention.

The following points characterize the threat from an ACH:

- there is virtually no upper limit to how hazardous the ACH can be;
- although estimates show that the average level of threat is low (for example, the probability for an Earth dweller being killed by an asteroid or comet impact is comparable to that of being killed in an air crash [3]), a specific event (impact) may have capital-C consequences, not only for an individual country, but for humankind as a whole;
- the threat is global in scope;
- unlike all other natural space-related threats, the global ACH threat can be predicted with a fairly high degree of certainty (provided the problems to be considered in Sections 2 and 3 are solved).

As a structurally complex problem (which it is), there are three basic aspects to be recognized in the ACH problem:

(1) Detecting, determining the properties of, and assessing the risk from hazardous celestial objects.

(2) Protection and damage reduction.

(3) Having a cooperative approach.

Problem number one for science — that of identifying all hazardous objects and determining their properties — is considered in Section 2. Section 3 discusses how to assess the impact consequences and general risk. Protection and damage reduction problems and work organization as a whole can hardly be ignored, even in a brief review like this, and they are accordingly addressed in Section 4, albeit in very general terms. Section 5 concludes and summarizes by pointing to the physical sciences — primarily astronomy and geophysics — as a key to solving the ACH problem.

2. How to detect and to obtain detailed knowledge of hazardous celestial objects

Before proceeding, some definitions are in order. By *near Earth objects* (NEOs) we refer to asteroids and comets with perihelion distance $q < 1.3$ AU. Among these, we distinguish *potentially hazardous objects* (PHOs) whose orbits can bring them within 7.5 million kilometers from Earth's orbit. The reason why an orbit away from the Earth's orbit in less than twenty Moon orbit radii makes an object a threat is that this distance is the scale of uncertainty which is involved in predicting the motion of a small celestial object 100 years or so in advance and which arises from the currently uncertain parameters and imperfect model describing the motion of the object.

The detection and detailed characterization of hazardous objects are at the top of the agenda for the ACH research community.

Detection, the way it is currently understood, means that a hazardous object (50 m or larger in size) needs to be detected promptly (no later than a month before a potential impact according to current requirements) and adequately (with a completeness greater than a certain threshold value, usually 90%). The subsequent regular *monitoring* of hazardous objects, both already known and those newly discovered by survey programs, should provide improved knowledge of their orbits and allow the full (as far as possible) study of their physical properties — potentially resulting in more

B M Shustov Institute of Astronomy, Russian Academy of Sciences, Moscow, Russian Federation
E-mail: bshustov@inasan.ru

Uspekhi Fizicheskikh Nauk **181** (10) 1104 – 1108 (2011)
DOI: 10.3367/UFNr.0181.201110e.1104
Translated by E G Strel'chenko; edited by A Radzig

Table 1. Impacts of small celestial objects with Earth: average rate and consequences.

Object	Size D	Characteristic intercollision interval	Crater size, km	Consequences of an impact with Earth
A small dust particle	$D < 0.1$ cm	Practically continuously		Burns up in the atmosphere or falls on the ground
Meteoroid	0.1 cm $< D <$ 1 m			Burns up in the atmosphere
	1 m $< D <$ 20–30 m	A few months		Reaches the ground at a low speed or completely disintegrates and burns up
	$D > 30$ m	About 300 years	None	Tunguska type mid-air explosion
			> 0.5	Ground explosion (for example, Arizona crater)
				Local catastrophe
Asteroid or comet	$D > 100$ m	Several thousand years	> 2	Ground or underwater explosion
				Regional catastrophe
	$D > 1$ km	More than 500 thousand years	> 2	Global catastrophe
	$D \approx 10$ km	100 million years	200	End of civilization

reliable evaluation of the probability and consequences of an impact and providing necessary information for humankind to take preventive measures in advance.

While until the mid-1990s hazardous objects were detected either by chance or within individual asteroid/comet research programs, the launch in 1998 of the Spaceguard Survey program supported (including financially) by the U.S. Congress, enabled detection at a much higher rate. In an important development, NASA committed itself to discovering, within ten years, no fewer than 90% of all near-Earth asteroids greater than 1 km in diameter — a task which is considered to have been completed by the end of 2009.

According to data from the NASA-funded Minor Planet Center operating under the auspices of the International Astronomical Union (http://cfa-www.harvard.edu/cfa/ps/mpc.html), about 8,000 NEOs had been discovered as of mid-April 2011 (overwhelmingly by US observation facilities and the US-coordinated network). Most of this number are asteroids; a few comets are a class of minor bodies which are very difficult to observe. According to data as of late June 2011, the number of PHOs is 1,237, including 70 comets.

The most important question is perhaps that of NEO detection completeness. Table 2 lists estimates of the number of 'unrecognized' potentially hazardous objects. There are an estimated few tens of thousands of PHOs more than 100 m in size and a few hundreds of thousands of PHOs more than 50 m in size. Quite uncertain as these estimates may be, the number of unrecognized objects is a hundred times that of known PHOs. What threatens us most is what we know of least!

Although there are quite a few large astronomical telescopes in the world, detecting PHOs on a mass scale is unfortunately not a task they are up to. A modern detection system requires developing special-purpose instruments. It is currently well known that, for a telescope to detect 50–100 m NEOs, the following parameters and operating conditions are optimum:

- a field of view of several (preferably ten) degrees squared;
- a penetrating power of 22nd stellar magnitude or more for exposures of no longer than a few dozen seconds, which implies a telescope aperture of no less than 1–2 m. Infrared (IR) space telescopes may have a smaller aperture, though, because it is mostly in the IR range (5–15 μm) that asteroids reradiate most of their absorbed solar energy;
- (for ground-based telescopes) a large number of clear nights and a high quality of images;
- very high-capacity computer equipment and mathematical software for obtaining operational information on new objects in one night and completely processing it before the next begins.

Table 2. The number of unrecognized potentially hazardous objects.

Size of the object, km	Estimated number of unrecognized PHOs	Proportion of unrecognized PHOs, %
> 1	< 40	< 20
> 0.140	$> 2 \times 10^4$	$\gtrsim 90$
> 0.05	$> 2 \times 10^5$	$\gtrsim 99$

There are a number of projects currently underway in the USA to develop instruments specialized to detect hazardous celestial objects. One of these, Pan-STARRS (Panoramic Survey Telescope and Rapid Response System) is primarily intended to solve the U.S. Air Force's space control problems.

The Pan-STARRS telescope, a system of four 1.8-m-aperture, 3-degree-field-of-view telescopes, has a charge coupled device (CCD) camera with a huge number (1.4 billion) of pixels and reaches a 24th stellar magnitude in 60 seconds. When in a search and survey mode, the entire available sky area is covered three times a month by these telescopes. As yet, only the first (prototype) telescope, PS1, has been built and is already in operation [4]. The still larger, 8-m LSST (Large Synoptic Survey Telescope) project is part of a unique civilian-purpose sky survey system [5] to be used for astronomical and cosmological purposes and for detecting dangerous objects. The system will be able to cover every 15 s a sky area 50 times that of the full Moon, and to detect objects as faint as 24.5th stellar magnitude. The telescope will have a 3-billion pixel digital camera and collect an equivalent of 7,000 DVDs of information nightly. The projected launch date of the facility is after 2015.

Radar observations of asteroids are of a great value not only in providing very accurate information on the orbital motion of an asteroid but also in providing data on its

physical properties, such as size, shape, and the composition of surface layers. The radar observation of individual asteroids is primarily conducted at the Goldstone and Arecibo radio astronomy observatories, at a rate of 10–15 objects per year [6] and with the radar range limited to 70 million km.

Russia, too, while lacking state-of-the-art equipment for the mass-scale detection of hazardous celestial objects, is making efforts to jump on the bandwagon. The wide-angle AZT 33VM telescope, a project of the Institute of Solar and Terrestrial Physics, Siberian Branch of the RAS (Irkutsk), with parameters only marginally worse than Pan-STARRS, appears to be the most promising. With a field of view of about 3 degrees and a primary mirror diameter of 1.6 m, AZT 33VM will be able to detect 24th stellar magnitude objects with an exposure time of 2 min.

Both in Russia and elsewhere, space-based NEO detection systems are being developed. These present major advantages over their Earth-based cousins and will already appear in space sometime within this current decade (for a more detailed discussion, see Ref. [1]).

The use of currently available astronomical instruments (or their networks) to monitor hazardous celestial objects is not so much a problem of technology as it is of organization. Thus far, no organizational 'interface' has been developed, which would allow these instruments (networks) to be used in the service mode, and it is precisely this mode — that is, a regular and standardized operation of observational systems involved — which is needed to solve ACH-related detection and monitoring problems.

The processing of information on the observed positions of NEOs is currently being carried out by the Minor Planet Center operating at the Smithsonian Astrophysical Observatory in Cambridge, MA, USA, which also identifies and assigns preliminary names to them, provides first preliminary and then more refined calculated results on their orbits, and publishes information on those objects for which additional observations are needed to confirm their discovery and to refine their orbits and other characteristics. The prediction of motion of potentially hazardous objects, the search for their close approaches to Earth, and the estimation of impact probabilities within the next few decades will be (and indeed are being) made at the Jet Propulsion Laboratory, Pasadena, CA, USA, and the University of Pisa, Italy.

In Russia, while a number of research institutes are concerned with exploring NEO motions, no measures have yet been taken on a systematic basis to achieve the country-wide integration of available information sources. The creation of a national information and analysis center for collecting and processing ACH-related information is at the top of the agenda.

3. Assessing risk

Assessing the degree of threat (or risk) is a crucial component of the ACH problem, because the underassessment or overassessment of risk leads to devastating consequences or huge material and social losses, respectively.

Two notions can be usefully introduced at this point: average impact risk, and a specific impact risk. The average degree of threat is calculated over a large time interval and, as we saw above, this background threat is moderate.

The degree of threat (risk) can be defined, to a first approximation, as the product of the impact probability and the severity of possible impact consequences. Although both are determined with a very large relative error, the risk must be evaluated opportunely and reliably. The reliable assessment of risk for a specific event (impact) and the timely delivery of an 'alarm signal' is what ACH science primarily is expected to provide — a task which requires a weighted and careful approach and which is another illustration of the high responsibility science has to society.

Put somewhat simplistically, the reliable assessment of risk factors is the responsibility of fundamental sciences: astronomy, in particular celestial mechanics, is expected to estimate the likelihood of a specific event (impact), whereas geophysics and physics of explosions, along with economic and social sciences, are responsible for assessing the impact consequences.

For risk assessment purposes, as far as PR is concerned, the so-called Torino scale is applied, which is similar to the white–red scale some countries use to categorize national threats. The Palermo scale, a more professional option introduced in Ref. [8], is the common logarithm of the relative risk R defined as $R = P_i(f_B \times DT)$, where P_i is the probability of a specific impact, DT is the time in years until the potential event, and f_B is the number of impact events per year with energy E (in TNT megatons) defined as $f_B = 0.03 \times E^{-4/5}$. That thus far no objects have been discovered to pose an alarmingly high level of risk is only due to our lack of knowledge. Whether applying the Torino or Palermo scale, the risk can be assessed only approximately. The calculation of a degree of threat for a specific impact is always individual in character.

Impact probabilities cannot currently be calculated without large errors. A review by the present author of some work on estimating the 2036 Apophis event risk revealed a spread in the calculated impact probabilities of as much as five (!) orders of magnitude. Clearly, to create a more reliable (certified) methodology, a critical overhaul is required, both of the mathematical methods used (in terms of their coordination) and in the description of the physical processes included in the models of motion.

Although time-proven approaches of classical celestial mechanics are of course being used to their full extent, even today there is still room for significant innovation in the field. A relatively recent example is the astronomical boom due to the widely recognized importance of the Yarkovsky effect and of its modification, the YORP (Yarkovsky–O'Keefe–Radzievskii–Paddack) effect for the evolution of asteroid orbits [10]. Some progress has also been made in calculating comet orbits, a very complex issue due to the large number of additional difficult-to-treat nongravitational factors (as exemplified by the fact that it is unrealistic, for a vaporizing comet, to calculate with high accuracy how the motion of its core is affected by the gas flow emerging from the core). This reasoning relates to the orbits of both the short-period and long-period comets. The appearance of the latters is currently unpredictable altogether.

Long-period comets are discovered at best a few months or a year before they appear in the vicinity of the Sun. As a typical example [11], for the comet C/1983 H1 (IRAS–Araki–Alcock), with an orbital period of 963.22 years, there was a mere two week gap between its discovery (27 April 1983) and its Earth flyby at a distance of 0.0312 AU (11 May 1983). Moreover, such comets have a large velocity relative to Earth, and their cores can disintegrate into large fragments. All this greatly complicates the problem of preventing comets from hitting Earth.

Along with the astronomical aspects, some of which have been considered above, of no less importance for developing adequate risk assessment methods is the accurate assessment of the consequences of a possible impact event. In doing such an assessment, a large number of specific factors should be considered, including the properties of the object, atmospheric entry conditions, the probable impact site, the date and time of the event, and ocean floor and beach profiles (an asteroid falling on sea can produce a tsunami!), plus adding a number of other important factors of an economic and social nature. Various aspects of the possible catastrophic consequences of an asteroid or comet hitting Earth are discussed in detail in monograph [12]. Note, however, that commonly accepted standards and procedures for reliably calculating risk are as yet unavailable, so efforts in this realm are clearly necessary. In this context, specialists from the Emergency Control Ministry of Russia (EMERCOM) and experts in natural disaster risk assessment have a crucial role to play (see, for example, Ref. [13]).

4. More aspects of the asteroid-comet hazard problem

The choice of measures to counter a space object impact threat should consider the size of the hazardous object and the warning time, i.e., the time available until the impact. There are two major methods to choose between destroying (disintegrating) the threatening object and deflecting (diverting) it from its orbit. If the warning time is large, say a few years or more, the current understanding favors the diversion scenario, whose implementation can be done in more than ten specific ways, according to experts.

In the short-warning low-mass case, breaking the object into smaller, nonthreatening pieces (using, for example, inertial mechanical dissectors) can be an option. For large masses, the only possible countermeasure is to disperse the object with nuclear (thermonuclear) explosions. An asteroid measuring more than 0.5 km across is a threat against which there is at present no defense. Importantly, the above methods need to be seriously worked out before being used. The consequences of an impact are still a matter of very large uncertainty. For more on that, see Ref. [1].

What is primarily needed to effectively address the ACH problem is cooperative efforts, both in Russia and internationally. In this context, the Expert Working Group on the Asteroid and Comet Hazard Problem was set up in 2007 at the Russian Academy of Sciences Council on Outer Space to coordinate research in this field in the country, which was transformed into the Expert Working Group on Space Threats early in 2011. The group comprised representatives from RAS research institutes, higher education institutions, the Russian Federal Space Agency (Roskosmos), EMERCOM, the Russian State Atomic Energy Corporation (Rosatom), the Russian Federation Ministry of Defense, and other interested agencies and organizations. Materials of the Expert Working Group are available at http://www.inasan.ru/rus/asteroid_hazard/.

The primary goal of the group was to conceptually develop an organizing program for a federal level ACH countermeasure system — somewhat analogous to the European Space Situational Awareness (SSA) program [14], under deployment since 2009.

The detection and monitoring of all hazardous objects, as well as their deflection (destruction) and the mitigation of damage they cause, are a challenge no country — even the most powerful one — can manage alone. The obvious areas where coordination is of particular importance are establishing a global network for detecting and monitoring hazardous objects and coordinating prevention and damage mitigation measures.

To prevent a threatening impact, an international decision-making procedure should be agreed upon and started under the aegis of the UN. In 2001, Action team 14 was established within the UN Committee on the Peaceful Uses of Outer Space for coordinating international efforts to address the ACH problem. The main task of the team is to prepare a document on interaction principles between states to be followed in organizing work on the ACH. A detailed discussion of the cooperation issue is given in Ref. [15].

5. Conclusion

This paper can obviously be summarized as follows:

(1) The ACH is quite a real problem and a serious global concern, and Russia cannot afford to sit on the sidelines.

(2) What science concerned with ACH has to provide first and foremost is reliable risk assessment for a specific event (impact) and a timely alarm signal. This requires a solid scientific approach and implies a very large responsibility to society.

(3) The physical sciences, particularly astronomy and geophysics, should play a dominant role in solving the ACH problem.

(4) The way things are in Russia, coordination on the part of the state is a sine qua non. For the project to be effective, a federal level program is needed.

References

1. Shustov B M, Rykhlova L V (Eds) *Asteroidno-Kometnaya Opasnost'* (Asteroid-Comet Hazard) (Moscow: Fizmatlit, 2010)
2. NASA. 2006 Near-Earth Object Survey and Deflection Study. Final Report, December 2006, http://www.hq.nasa.gov/office/pao/FOIA/NEO_Analysis_Doc.pdf
3. Morrison D et al., in *Asteroids III* (Eds W F Bottke (Jr.) et al.) (Tucson, AZ: Univ. of Arizona Press, 2002) p. 739
4. Chambers K C *Bull. Am. Astron. Soc.* **41** 270 (2009)
5. Ivezić Ž et al. *Serb. Astron. J.* (176) 1 (2008)
6. Ostro S J, Giorgini J D, Benner L A M, in *Near Earth Objects, Our Celestial Neighbors: Opportunity and Risk* (Proc. IAU Symp. 236, Eds G B Valsecchi, D Vokrouhlický, A Milani) (Cambridge: Cambridge Univ. Press, 2007) p. 143
7. Denisenko S A et al. *Opt. Zh.* **76** (10) 48 (2009) [*J. Opt. Technol.* **76** 629 (2009)]
8. Chesley S R et al. *Icarus* **159** 423 (2002)
9. Neukum G, Ivanov B A, in *Hazards due to Comets and Asteroids* (Eds T Gehrels, M S Matthews, A Schumann) (Tucson, AZ: Univ. of Arizona Press, 1994) p. 359
10. Bottke W F (Jr.) et al. *Annu. Rev. Earth Planet. Sci.* **34** 157 (2006)
11. Huebner W F et al. *Solar Syst. Res.* **43** 334 (2009)
12. Adushkin V V, Nemchinov I V (Eds) *Katastroficheskie Vozdeistviya Kosmicheskikh Tel* (Catastrophic Events Caused by Celestial Objects) (Moscow: Akademkniga, 2005)
13. Akimov V A, Lesnykh V V, Radaev N N *Riski v Prirode, Tekhnosfere, Obshchestve i Ekonomike* (Risks in Nature, Technosphere, Society and Economy) (Moscow: Delovoi Ekspress, 2004)
14. Bobrinsky N, Del Monte L *Kosmicheskie Issled.* **48** 402 (2010) [*Cosmic Res.* **48** 392 (2010)]
15. Shustov B M *Kosmicheskie Issled.* **48** 388 (2010) [*Cosmic Res.* **48** 378 (2010)]

PACS numbers: **11.27.+d**, 98.62.Sb, 98.80.Es
DOI: 10.3367/UFNe.0181.201110f.1109

Search for cosmic strings using optical and radio astronomy methods

O S Sazhina, M V Sazhin, M Capaccioli, G Longo

1. Introduction

The last decade has seen an active search for cosmic strings by the methods of observational astronomy: both in optical and in radio surveys. The splash of this research is due, on the one hand, to significant progress in the area of investigations into the multidimensional structure of space-time and in the search for theories claiming to be the unified theory of all physical interactions. On the other hand, studies of the extragalactic object CSL-1 carried out by a joint Russian–Italian group made it possible for the first time to lay and develop the observational basis for the quest for cosmic strings by gravitational lensing techniques. Lastly, the rising accuracy of measuring the anisotropy of cosmic microwave background radiation (CMBR) [data of the processing of the seven-year-long observations in the WMAP (Wilkinson Microwave Anisotropy Probe) space mission, and data from the Planck space observatory] gives a good chance to find an unambiguous solution to the question of the existence of cosmic strings in a wide mass range.

According to modern observational data on the expansion of the Universe, obtained by studying supernovas, and to data on the anisotropy of CMBR, the Universe now resides at the stage of accelerated expansion, which is successfully explained by the existence of dark energy — a special form of a vacuum type energy [1]. However, the nature of dark energy has not been elucidated, which is a fundamental problem of modern cosmology and the key area of research at the interface between such disciplines as cosmology, astronomy, and elementary particle physics.

In the framework of this problem, of special interest is the investigation of dark energy of the early Universe, specifically, of possible soliton and soliton-like solutions. Stable one-dimensional structures — cosmic strings (CSs), which emerge in all the most realistic models of elementary particle physics — represent such a solution [2, 3]. Modern research in elementary particle physics gives ample evidence of the existence of new physics beyond the framework of the Standard Model. CSs emerge both in the models of Grand Unification and in superstring theory [4, 5]. Not only would the discovery of CSs permit revealing the nature and evolution laws of the dark energy of the early Universe, but it would also make it possible to study an energy scale unattainable with modern accelerators.

CSs, which were first predicted by T Kibble in 1976, were actively studied in subsequent papers by Ya Zeldovich and by A Vilenkin and E Shellard [3, 6–9]. The existence of CSs is not at variance with all the presently available cosmological observational data and, furthermore, is gaining support from the theory and receiving indirect confirmation from observations.

O S Sazhina, M V Sazhin, M Capaccioli, G Longo Sternberg Astronomical Institute, Moscow State University, Moscow, Russian Federation
E-mail: tedeshka@mail.ru

Uspekhi Fizicheskikh Nauk **181** (10) 1109 – 1114 (2011)
DOI: 10.3367/UFNr.0181.201110f.1109
Translated by E N Ragozin; edited by A Radzig

2. Cosmic string in the Universe

2.1 Main definitions and properties

From the observational point of view, of greatest interest are topological CSs (solitons), since the mechanism of their formation (phase transitions of the vacuum) is rather simple and has been much studied experimentally in other areas of physics (transitions in ferromagnetics, the superconductivity phenomenon, etc.). Furthermore, this mechanism of string formation does not require special assumptions about dynamic processes in the Universe and is primarily based on the fact that the early Universe was higher in temperature than the contemporary one and cooled in its evolution.

The formation of topological defects with various dimensions is due to the fact that the vacuum manifold in the theory is structurally nontrivial: $\pi_N(M) \neq 0$. When space-time has a dimension $d+1$, it may contain topological defects with a dimension $d-N$: monopoles, strings, domain walls, as well as hybrid defects, for instance, 'necklaces' (monopoles and strings) and fleece (strings and walls). In the case of strings, one has $N=1$, and the nontriviality of the homotopy group $\pi_1(\mathrm{S}^1)$ signifies the existence of circumferences which cannot be contracted to a point by a continuous transformation.

The minimal string-containing model possesses a U(1)-gauge-invariant Lagrangian density [1]

$$L = D^{\mu}\phi^{*} D_{\mu}\phi - \frac{1}{4} F_{\mu\nu} F^{\mu\nu} - \lambda\left(\phi^{*}\phi - \frac{T_{\mathrm{c}}^2}{2}\right)^2 .$$

The ground state of this model is not gauge-invariant with respect to the U(1) group. The nonzero vacuum manifold is determined by the characteristic energy scale T_{c}. The potential reaches its minimum on a circumference:

$$\langle\phi\rangle = \frac{T_{\mathrm{c}}}{\sqrt{2}} \exp\left[\mathrm{i}\alpha(x)\right] .$$

For $T \leqslant T_{\mathrm{c}}$, the symmetry of the ground state is broken and in every causally coupled space-time domain the value of phase $\alpha(x)$ is fixed — the system changes to one of the energy preferred states in a random manner. Clearly, the phases in each of these domains do not correlate. Owing to the unambiguity of field ϕ, the phase variation along a closed path passing through different causally disconnected domains is expressed as $\Delta\alpha = 2\pi N$. When $N \neq 0$, a CS forms with a conserved topological charge N (N is the number of winds). The field ϕ, owing to its continuity, should assume a zero value inside of the phase variation path. Therefore, the new-phase domain encloses the old — 'relic' — phase domain. This mechanism of topological CS formation is termed the Kibble mechanism.

The continuity of field ϕ also ensures the finiteness of string energy: the string is stable, having no ends in the causally coupled domain of space-time — it either 'pierces' through the horizon or forms loops. Long strings tend to straighten, and the loops tend to collapse. Simulations also show that 80% of the strings are long [10–12]. The below-proposed methods of searching for CSs are aimed at the search for straight segments of long individual strings.

The main parameter of a CS is its linear density $\mu = \mathrm{d}E/\mathrm{d}z = \pi T_c^2$. For convenience, one can introduce a dimensionless parameter $G\mu \propto (T_c/M_{Pl})^2$. For most realistic CSs, those with energies of about $10^{15}-10^{16}$ GeV, the quantity $G\mu \propto 10^{-7}-10^{-6}$. Also, the linear density of the string is conveniently estimated using parameter $\mu_6 \approx 0.1-1$ [4] as $\mu = 1.35 \times 10^{21}\mu_6$ [kg m^{-1}] $= 2.09 \times 10^7 \mu_6 M_\odot$ [pc^{-1}].

2.2 Place of cosmic strings in modern physics

Recent investigations [4, 5, 13] have revealed tight theoretical interrelations between topological CSs and the fundamental superstring theory, which presently are the most promising candidates for the construction of matter and the unification of all types of physical interactions. This interrelation was made possible by the mechanisms of energy lowering for the strings of the fundamental theory.

The linear density of a string is proportional to the square of the temperature of the corresponding phase transition. For a CS, one has $G\mu \leqslant 10^{-6}$. For superstrings, $\mu \propto M_s^2$, and $G\mu = M_s^2/M_{Pl}^2 \approx 1$. In models with extra noncompact dimensions, the superstring energy scale may be lowered: $M_s \ll M_{Pl}$, which results in $G\mu \ll 1$. In models with a large fifth dimension (four-dimensional bran and bulk models), the superstring energy may also be lowered because a part of the string energy is transferred to the bulk.

Nontopological superstrings (so-called F- and D-strings) might have been formed in the early Universe. Observations of such objects could be the main way of studying fundamental superstrings. These objects are predicted by the newest models with extra noncompact dimensions (the process of bran–antibran annihilation) and by a broad class of inflation cosmological models. It has been established during the last several years that a vast family of CSs exists, which differ in properties, these properties being directly dependent on the geometry of the extra compactified dimensions of superstring theory.

As is well known, the key problem of modern multidimensional theories is that there is no way of giving preference of one theory to another — only observational facts, like the discovery of a CS, could sort out unrealistic theories and bring the modern physics of elementary particles to a radically new level. Furthermore, the discovery of CSs would yield information about the composition of the relic dark energy of the early Universe, which would allow making rapid strides towards understanding the reasons for the contemporary accelerated expansion of the Universe, which is governed by a yet unknown type of dark energy.

Among all possible types of topological defects, only CSs emerge in a natural way in the overwhelming majority of realistic models of the early Universe. CSs may exist in a broad mass range: from the energies of grand unified theories to those of electroweak theory.

2.3 Main properties of a cosmic string as an object of observations

The methods of searching for CSs rely on their special properties which are different from the properties of all known types of celestial objects. We shall indicate these properties by the simple model example of the Euclidean universe with a single string inserted in it [7, 14]. In the consideration of the real Friedmann–Robertson–Walker (FRW) cosmological model and of several strings, these properties will qualitatively persist. In a specially selected coordinate system [14], the metric of space-time with a string is conical. This metric coincides everywhere with the Minkowski metric

$$g_{\mu\nu} = \eta_{\mu\nu} = \mathrm{diag}\,(1, -1, -1, -1)$$

with the exception of one point — the vertex of the cone. For any circumference containing the vertex of the cone, the length-to-radius ratio equals $2\pi - \alpha$, where α, termed the deficit angle, is determined by the linear density of the string: $\alpha = 8\pi G\mu$. Everywhere, with the exception of the cone vertex, the space is Euclidean (Fig. 1).

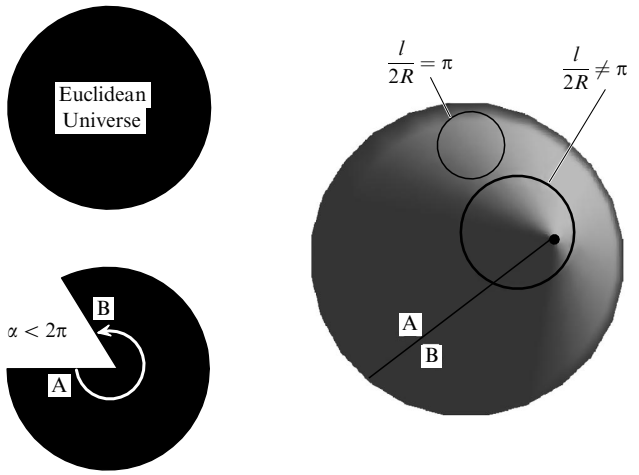

Figure 1. Illustration of the formation of a conical universe in the presence of a single cosmic string.

A straight CS does not possess a gravitational field. Nevertheless, the existence of a cut makes possible the formation of gravitationally lensed images of objects which are background relative to the string. Moving along straight lines, the light rays emanating from the background source nevertheless skirt the cone vertex to form images. The essential one-dimensionality of the CS dictates several special properties of such images. The string's one-dimensionality also manifests itself in a unique manner in the investigation of CMBR anisotropy which may be generated by a moving CS.

2.4 Current status of cosmic strings in observational cosmology

There are several methods for the observational search for CSs, which may be conventionally divided into three groups. The first method — finding strings by optical surveys — consists in the search for characteristic gravitational lensing events occurring in the lensing of background sources (primarily galaxies) by the strings. The second one involves investigations into the structure of CMBR anisotropy induced by strings, and the determination of the characteristic amplitudes of these structures. The third method implies the search for a large number of low-probability and model-dependent string manifestations, like the emission of gravitational waves by string loops, string–black hole interactions, decay of heavy particles emitted by strings, and the interactions between two or more strings. Only the first two methods are universal for all string types and will be the subject of our consideration.

The latest data on the anisotropy of CMBR rule out CSs as the source of primary density perturbations but do not forbid their existence. The previously employed statistical methods of analysis of CMBR anisotropy enable revealing strings which produce an anisotropy of no less than 100 μK [15]; no strings have been found by these methods. Selective searches (optical catalogs covering 1/6 of the celestial sphere) for gravitational lensing events for a string deficit angle of no less than 2″ have not met with success, either.

3. Effect of gravitational lensing by a cosmic string

3.1 Gravitational lensing of point and extended sources by a cosmic string

By analogy with how this is done in the modeling of classical gravitational lensing events, we define three parallel planes: the plane of a point source I $\{\xi, \eta\}$, the string–lens plane $\{x, y\}$, and the observer's plane. Let R_g be the distance between the observer's plane and the source plane, and R_s be the distance from the observer's plane to the lens plane. In each plane, the origin lies in the straight line passing through the observer perpendicular to all the three planes. When the source I is in the band $\delta\theta = \alpha(R_g - R_s)/R_g$, where $\alpha = 8\pi G\mu$, two images spaced at physical distances D_ψ and D_ϕ from the origin are formed in the string–lens plane (Fig. 2). The problem of the gravitational lensing of a point source involves finding these distances as functions of the position of source I in the $\{\xi, \eta\}$ plane, deficit angle α, and distances R_g and R_s between the planes [16].

The case of an extended source is investigatively similar [16]. The solution is sought for as the result of lensing of the set of point sources. The image exhibits clearly defined isophot cuts (Fig. 3).

Therefore, gravitational lensing by a CS is characterized by the presence of a chain of the image pairs of sources which are background relative to the string. The spacing between the images in each pair is determined by the string deficit angle. For instance, an angular distance of 2″ corresponds to a string energy on the order of 10^{16} GeV. Furthermore, when the background objects are optically resolved, the structure of the outer isophots of image brightness should exhibit characteristic cuts, which is due to the essential one-dimensionality of the string. To observe suchlike cuts requires, as a rule, high angular resolution, on the order of 0.1″.

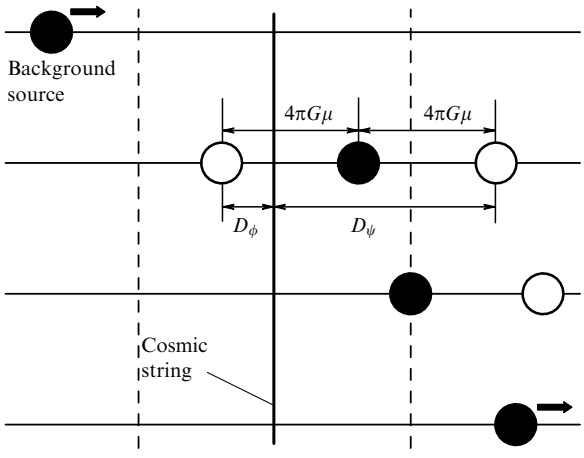

Figure 2. Simulation of the gravitational lensing of a moving point source by a cosmic string viewed in the plane of the string. The string is parallel to the plane of the drawing.

Figure 3. Simulation of the gravitational lensing of an extended source (a galaxy) by a cosmic string viewed in the plane of the string. The string is parallel to the plane of the drawing. One can see the cuts of outer isophots of the source. Angular resolution is 0.1″.

3.2 Investigation of object CSL-1

In 2003, a deep survey by the INAF's Astronomical Observatory of Capodimonte (Naples, Italy) resulted in the discovery of a pair of objects, which was termed CSL-1 and had supposedly gravitational lensing origin [17, 18]. This conclusion was drawn on the basis of spectroscopic and photometric analysis of this pair of objects: both components possessed a zero difference of radial velocities and the same brightness profiles, being resolved in this case. The spectra of both components are identical to an accuracy exceeding 99%. No tidal distortions were observed, either. The absolute stellar magnitude of both components (with filter R) is −22.3. The components of the pair are spaced at 1.9″, and the red shift is 0.46. The distance to the observer is about 1.9 Gpc.

Being supposedly a gravitationally lensed object, CSL-1 showed no characteristic arc-like distortions of the outer isophots. The phenomenon of gravitational lensing of galaxies by other objects (galaxies, groups of galaxies, etc.) is not infrequent in our Universe. However, the uniqueness of the CSL-1 double object consists in the fact that the only type of a gravitational lens which can produce observable morphologically identical undistorted images is a CS. For a classical gravitational lensing of a background galaxy by known cosmic objects, owing to the nonuniformity of gravitational fields of the latters, the images of the background galaxy are significantly distorted. The gravitational potential of a straight CS is equal to zero, and so the resulting images are undistorted. Acting as a gravitational lens, a CS forms a conical space wherein the light rays from the background galaxy pass relatively along opposite sides of the cone vertex to form two images.

Therefore, the lens forming this pair of images must have a one-dimensional structure, which is evidence of a CS. Simulations demonstrated that lensing by the CS corresponds to the real data acquired by the ground-based

telescopes TNG (Telescopio Nationale Galileo), NTT (New Technology Telescope), and VLT (Very Large Telescope) at a 2σ confidence level. Specifically, the processing of images showed that the spectra of objects in the pair are highly correlated (for a thousand points the correlation coefficient reached 0.85, and in this case it was *a priori* assumed that both components are elliptical galaxies and possess equal spectrum slopes; this dependence did not enter into the correlation coefficient). The difference between the spectra of the two components represented random noise with an autocorrelation function close to unity.

This spectral identity suggested that there was a dust bar passing along the middle of one strongly prolate elliptical galaxy. Furthermore, in order for two circular sources to be formed eventually, the bar had to possess the strongly pronounced shape of an hourglass. This exotic hypothesis, which nevertheless had the right to exist, was refuted by observations with an infrared filter on the 3.5-meter Galileo National Telescope in 2003. The point is that dust should be transparent in the infrared range for a conventional dust absorption law. Moreover, the absorption coefficient is wavelength-dependent for any dust absorption law, and therefore the dust bar should be different in appearance with different filters, which was not observed for the CSL-1 object. The 2005 observations with the VLT telescope system of the European Southern Observatory (ESO) located on the Paranal Plateau in Chile confirmed the identity of the spectra of both components of the pair with an even higher accuracy (99.9%).

Apart from gravitational lensing interpretation, there persisted, as before, a nonzero probability that CSL-1 comprises two different galaxies spaced at a projection distance of less than 10 kpc. Clearly, the physical distance between them should be longer; otherwise, it would have been possible to observe tidal effects for the 10% photometric accuracy involved. On the other hand, the distance should not be too long; otherwise, the galaxy more distant from the observer would be lensed by the closer one, which was not observed, either. In view of the zero difference between radial velocities, the length of admissible physical distance between the galaxies lowered to only 15 Mpc. On raising the photometric observational accuracy to 0.1%, the interval of intergalactic distances is further lowered almost threefold, to 123 kpc – 5 Mpc, which is hardly probable in view of the same morphology of the two resolved components of the pair and the identity of their spectra. Therefore, the hypothesis of the gravitational lensing origin of CSL-1 prevailed.

Our group also obtained additional arguments in favor of the CS-based explanation of the CSL-1 phenomenon. They consist in the discovery of candidates for gravitational lensing events in the vicinity of CSL-1, as predicted by the theory. Using comprehensive photometric data gathered with different color filters, it was possible to discover 11 such candidates, whose gravitational lensing nature had to be verified with the ESO VLT telescope in future projects. Also submitted were applications for observations with the newest VLT Survey Telescope (VST)—a general survey telescope for the ESO VLT, a project of the Astronomical Observatory of Capodimonte. The VST telescope enables collecting a huge amount of photometric data, including those from very weak sources (up to the 25th stellar magnitude with the R filter). This would allow validly using this instrument for investigating the CSL-1 object and the candidates for gravitational lensing events, most of which are weak sources (from the 19th to 24th stellar magnitude).

Observations with the NASA's Hubble Space Telescope performed on 11 January 2006 helped to finally solve the question about the nature of this mysterious binary object. Six satellite orbits were allocated to our project, and observations were carried out with a resolution of 0.05″ for about 14,000 s. To interpret the observational data, numerical simulations were made of the gravitational lensing of a background object by a CS, and analytical equations were derived for a gravitational lens.

According to theoretical calculations, if lensing by a CS occurs, there must be no isophot distortions for an extended background source (which emerge in its lensing by an extended object), the spectra of the objects in the pair should be identical, and the radial velocity difference should be equal to zero. All these requirements were met for the CSL-1 object. In the case of lensing by a CS and the high angular resolution attainable with the HST, characteristic cuts of outer isophots should be observable in the background source images. Furthermore, structure doubling should be observable: for instance, when some morphological features are present in one image and its vicinity with a size smaller than or equal to the linear dimension of the string deficit angle, they are bound to be present in the second image as well.

Yet another indication of string existence is a chain of object pairs which also possess the characteristic cuts of outer isophots. The separation of the objects in each pair must not exceed the linear dimension of string deficit angle. The gravitational lensing effect begins to show up as soon as the background source comes into the vicinity-belt of action of the string, whose width is determined by the string deficit angle; while in the case of a two-galaxy projection effect there are bound to be observable tidal distortions for the HST resolution. The HST observations showed that there is a weak tidal interaction between the two elliptic galaxies which were unobservable for ground-based telescopes.

Therefore, the question about the nature of the CSL-1 double object was finally elucidated: it is an extremely rarely occurring gravitationally coupled system of two galaxies (Fig. 4).

Despite the fact that the hypothesis of a CS was not confirmed, the investigation carried out made it possible to

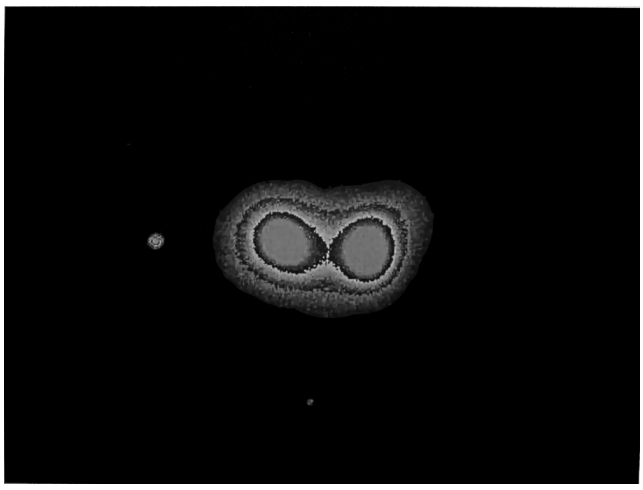

Figure 4. CSL-1 object. Image from the Hubble Space telescope. One can see tidal distortions of outer isophots.

develop for the first time the complete theory of the gravitational lensing of extragalactic objects by a solitary straight CS, to reveal all possible observational manifestations of the CS, and to calculate the required characteristics and resources of the ground-based and space instruments needed for conducting these investigations. The results obtained are actively being used by the world scientific community (see Refs [19, 20] and references cited therein).

4. Relic radiation anisotropy induced by a cosmic string

The last three years have observed investigations of CMBR anisotropy generated by a CS (see Refs [14, 21] and references therein).

According to the findings of our research, a moving straight CS should generate characteristically shaped structures with enhanced and reduced brightness. The anisotropy structure comprises a sequence of regions with lower and higher temperatures: specifically, a cold spot ahead of the CS motion front, then a pronounced temperature step and a hot spot, which is replaced with a cold spot again (Fig. 5).

To be certain about the discovery of a string with the employment of this technique, independent observations of the same region in the sky should be carried out in another frequency region. The quest for gravitational lensing effects would be the best observation of this kind. It is significant that the characteristic CS length should be great, no less than 100°, if the CS is to be simultaneously observable in the optical range and in the radio frequency band. This magnitude stems from the fact that only relatively close objects with a red shift $z \leqslant 7$ are accessible to optical observations, while for CMBR one has $z \approx 1000$. Hence, it follows, in particular, that the number of cosmic strings which may be discovered by purely optical methods of observation amounts to only 20% of the total number of strings in the Universe. This fact provides for the first time an explanation for the failure to discover a CS by exploring gravitational lensing effects.

The following simple model was considered in Ref. [14]. An observer is located at the center of the sphere $\{O, \xi, \eta, \zeta\}$. The sphere radius is the distance to the surface of the last scattering. The sphere may be assumed to be nonexpanding to a sufficient accuracy. A straight string is moving with velocity v at an angle ψ perpendicular to the plane $\{O, \xi, \eta\}$, piercing the sphere at points A and B. The CMBR anisotropy produced by the string is caused by the Doppler effect. The temperature fluctuation takes on the form

$$\delta T = 27 \, \frac{\alpha}{2''} \, \frac{\beta}{0.9} \, F(\psi, \phi, \theta) \ [\mu\mathrm{K}] .$$

The contribution of the string velocity to the Doppler effect is made only by the quantity β — the projection of the string velocity (in units of the speed of light) onto the axis perpendicular to the line of sight. The function of spherical angles reduces to $F(\psi, \phi, \theta) \approx 1$.

The anisotropy structure is independent of the magnitudes of model parameters. For a relativistic $(v/c \approx 1)$ CS possessing an deficit angle of about $1-2''$, the amplitude of the generated anisotropy is of order (15–30) μK.

If a CS is to be searchable both by optical gravitational lensing techniques and by the analysis of CMBR anisotropy, the deficit angle should range from several tenths of an arc second $(\delta T/T \approx 1.5)$ to $5-6''(\delta T/T \approx 100)$. The lower bound is defined by the highest resolution attainable in the optical region (by HST) in the quest for string-induced galactic gravitational lensing events. The upper bound gives a magnitude of string anisotropy comparable to the standard anisotropy caused by adiabatic density perturbations.

The signal delay effect [22], which is caused by the string extent, should also be taken into account: when an infinitely long straight string is moving some distance away from the observer, they see different parts of the string at different instants of time.

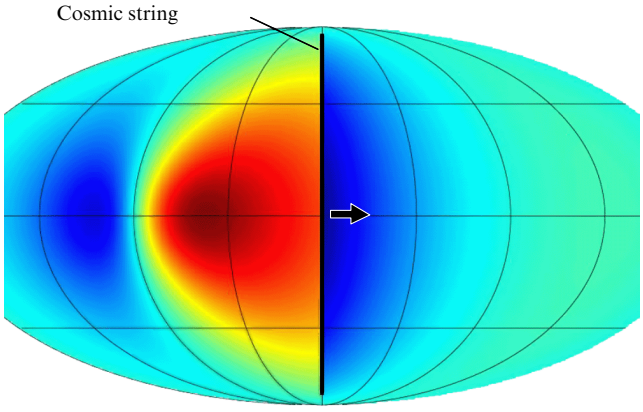

Figure 5. Simulation of CMBR anisotropy generated by a moving straight cosmic string. Mollweide projection of celestial sphere. The string is parallel to the plane of the drawing, coincides with the axis connecting the poles, and moves from left to right. Characteristic structure of the anisotropy: a cold spot ahead of the front, a delta-like temperature step, a hot spot behind the front, and a cold trailing spot.

5. Conclusions

The following investigations have made significant contributions to the progress of observational methods in the quest for CSs.

The binary extragalactic CSL-1 source was discovered and explored. Observations from the HST in 2006 were able to refute the CS hypothesis by showing that a projection effect occurs for two galaxies with similar morphologies and spectra, which possessed close peculiar velocities. Nevertheless, the meticulous theoretical and observational work carried out enabled for the first time constructing a rather complete model of the gravitational lensing of background objects by a CS as applied to real observations, especially those reliant on instruments with a high angular resolution.

A study was made of the Q0957+561A, B quasar. Anomalous brightness fluctuations were discovered in the gravitational lensing system; one of the possible reasons for their occurrence is the gravitational lensing effect by a cosmic CS.

New evidence for the presence of a CS was found in the WMAP satellite data on the anisotropy of CMBR generated by a uniformly moving straight CS. The number of strings which can be found by optical methods amounts to 20% of their total number, i.e., the quest for them in the optical range should be necessarily complemented with analysis of the radio maps of CMBR anisotropy. For strings with an deficit angle of $1''-2''$, the generated anisotropy amplitude ranges 15–30 μK [for strings with the most realistic energies $(10^{15}-10^{16}$ GeV) and the corresponding densities $(G\mu \propto 10^{-7}-10^{-6})$]. If a string is to be detected

by two independent methods (optical and radio methods), the CS deficit angle should lie in the range between $0.1''$ and $5-6''$. When a CS is detectable by optical methods, the characteristic 'spot' size on the anisotropy map should be no less than 100°.

The fields of the HST (4.5 square degrees in all) were studied in the search for gravitationally lensed pairs formed by straight long CSs. Four candidates for CS-induced gravitational lenses were discovered; however, the accuracy accessible to researchers is not high enough to unambiguously elucidate the nature of these candidates.

Acknowledgments. This work was supported by a grant No. 10-02-00961a from the Russian Foundation for Basic Research, and a grant No. MK-473.2010.2 from the President of the Russian Federation. This work was performed under the auspices of the Ministry of Education and Science of the Russian Federation (project No. 14.740.11.0085).

References

1. Gorbunov D S, Rubakov V A *Vvedenie v Teoriyu Rannei Vselennoi: Teoriya Goryachego Bol'shogo Vzryva* (Introduction to the Theory of the Early Universe: Hot Big Bang Theory) (Moscow: URSS, 2008) [Translated into English (Singapore: World Scientific, 2011)]; *Vvedenie v Teoriyu Rannei Vselennoi: Kosmologicheskie Vozmushcheniya, Inflyatsionnaya Teoriya* (Introduction to the Theory of the Early Universe: Cosmological Perturbations and Inflationary Theory) (Moscow: URSS, 2010) [Translated into English (Singapore: World Scientific, 2011)]
2. Hindmarsh M, in *The Formation and Evolution of Cosmic Strings: Proc. of a Workshop Supported by the SERC and Held in Cambridge, 3–7 July, 1989* (Eds G W Gibbons, S W Hawking, T Vachaspati) (Cambridge: Cambridge Univ. Press, 1990) p. 527
3. Vilenkin A, Shellard E P S *Cosmic Strings and Other Topological Defects* (Cambridge: Cambridge Univ. Press, 1994)
4. Davis A-C, Kibble T W B *Contemp. Phys* **46** 313 (2005); hep-th/0505050
5. Copeland E J, Myers R C, Polchinski J *JHEP* (06) 013 (2004); hep-th/0312067
6. Kibble T W B *J. Phys. A Math. Gen.* **9** 1387 (1976)
7. Vilenkin A *Phys. Rev. D* **23** 852 (1981)
8. Vilenkin A *Astrophys. J. Lett.* **282** L51 (1984)
9. Zeldovich Ya B *Mon. Not. R. Astron. Soc.* **192** 663 (1980)
10. Allen B, Shellard E P S *Phys. Rev. Lett.* **64** 119 (1990)
11. Uzan J-P, Bernardeau F *Phys. Rev. D* **63** 023004 (2001); Bernardeau F, Uzan J-P *Phys. Rev. D* **63** 023005 (2001)
12. de Laix A A, Vachaspati T *Phys. Rev. D* **54** 4780 (1996)
13. Majumdar M, hep-th/0512062
14. Sazhina O S, Sazhin M V, Sementsov V N *Zh. Eksp. Teor. Fiz.* **133** 1005 (2008) [*JETP* **106** 878 (2008)]
15. Lo A S, Wright E L, astro-ph/0503120
16. Sazhin M V et al. *Mon. Not. R. Astron. Soc.* **376** 1731 (2007); astro-ph/0611744
17. Sazhin M et al. *Mon. Not. R. Astron. Soc.* **343** 353 (2003)
18. Sazhin M V et al., astro-ph/0601494
19. Morganson E et al. *Mon. Not. R. Astron. Soc.* **406** 2452 (2010)
20. Gasparini M A et al. *Mon. Not. R. Astron. Soc.* **385** 1959 (2008)
21. Stebbins A *Astrophys. J.* **327** 584 (1988)
22. Vilenkin A *Nature* **322** 613 (1986)

PACS numbers: **04.20.–q**, **97.82.–j**, 98.62.Sb
DOI: 10.3367/UFNe.0181.201110g.1114

Search for exoplanets using gravitational microlensing

A F Zakharov

1. Gravitational lensing: introduction

There are different regimes of gravitational lensing depending on the mass of the gravitational lens. Assuming that both the lens and the source are located at cosmological distances, different regimes correspond to different angular distances between images. The case of a stellar-mass gravitational lens is referred to as gravitational microlensing. The angular distance between images in this case is proportional to the square root of the lens mass, so the lensing of a planet with a mass a few times smaller than Earth's ($10^{-6}M_\odot$, where $M_\odot$ is the solar mass) is called nanolensing.

Thus, searches for sufficiently light exoplanets using gravitational lensing can be dubbed gravitational nanolensing. Different methods of searches for exoplanets are known, including the Doppler shift of spectral lines, transits, and pulsar timing. In this paper, we show that gravitational microlensing is one of the most promising methods of searching for Earth-like exoplanets (with masses of order $M_\oplus$) located at distances of several astronomical units (AU) from a star, and there is hope that exoplanets with a solid surface temperature in the range $1-100\,^\circ$C (i.e., with the temperature of liquid water) can be discovered.

A detailed discussion of gravitational lensing can be found in monograph [1] (see also review [2]). Nevertheless, we shall remind the reader of the basic facts and report on new results in this field.

Gravitational lensing is based on the gravitational light bending effect. It can be visualized as if a gravitating body attracts photons. Gravitational light bending was first discussed by Sir Isaac Newton [3]. Such a bending appears to be the natural conclusion from the corpuscular theory of light advocated by Newton. A derivation of the light deflection angle in Newtonian gravity was first published by the German astronomer Johann Georg von Soldner [4].

In General Relativity (GR), the light deflection angle in the gravitational field was obtained by Albert Einstein [8]:

$$\Theta = \frac{4GM}{c^2 p}\,, \tag{1}$$

where M is the mass of the gravitating body, p is the impact parameter, c is the speed of light in vacuum, and G is the Newtonian constant of gravitation. If $M = M_\odot$ and $p = R_\odot$ (where $R_\odot$ is the solar radius), the respective light deflection angle is $1.75''$. In 1919, this prediction was confirmed by

A F Zakharov Russian Federation State Scientific Center
'A I Alikhanov Institute for Theoretical and Experimental Physics', Moscow, Russian Federation
Joint Institute for Nuclear Research, Dubna, Moscow region, Russian Federation
E-mail: zakharov@itep.ru

Uspekhi Fizicheskikh Nauk **181** (10) 1114–1122 (2011)
DOI: 10.3367/UFNr.0181.201110g.1114
Translated by K A Postnov; edited by A Radzig

measuring the displacements in coordinates of stars near the solar limb during the total solar eclipse of May 29. The observations were carried out in Príncipe island (near South Africa) and in the village of Sobral in northeast Brazil [6]. During several subsequent decades, nevertheless, observers checked the predictions of GR and sometimes came to the conclusion that these predictions were in disagreement with experiment (for example, the measurements of the star displacements carried out by E Freundlich in Sumatra Island during the total solar eclipse in 1929). Nevertheless, by the middle of the 1950s it was concluded that observations of light bending in the gravitational field generally corresponded to theoretical predictions [7].

Using formula (1), one can derive the gravitational lens equation:

$$\boldsymbol{\eta} = \frac{D_\mathrm{s}\boldsymbol{\xi}}{D_\mathrm{d}} - D_\mathrm{ds}\boldsymbol{\Theta}(\boldsymbol{\xi}), \tag{2}$$

where D_s, D_d, and D_ds are the respective distances between the source and the observer, the lens and the observer, and the source and the lens. Vectors $\boldsymbol{\eta}$ and $\boldsymbol{\xi}$ determine the coordinates in the source and the lens planes, respectively:

$$\boldsymbol{\Theta}(\boldsymbol{\xi}) = \frac{4GM\boldsymbol{\xi}}{c^2\xi^2}. \tag{3}$$

If the source, lens, and observer are located along one straight line, the right side of Eqn (2) must vanish ($\boldsymbol{\eta} = 0$), and then, by substituting $\boldsymbol{\Theta}$ from Eqn (3) into Eqn (2), we obtain the so-called Einstein–Chwolson radius [1] [11]

$$\xi_0 = \sqrt{\frac{4GMD_\mathrm{d}D_\mathrm{ds}}{c^2 D_\mathrm{s}}} \tag{4}$$

and, correspondingly, the Einstein–Chwolson angle determined by the relation $\theta_0 = \xi_0/D_\mathrm{d}$. If $D_\mathrm{s} \gg D_\mathrm{d}$, then

$$\theta_0 \approx 2'' \times 10^{-3}\left(\frac{M}{M_\odot}\right)^{1/2}\left(\frac{D_0}{D_\mathrm{d}}\right)^{-1/2}, \tag{5}$$

where $D_0 = 1$ kpc.

1.1 Gravitational lensing regimes

There are many reviews and monographs devoted to gravitational lensing and microlensing [1, 11–15]. Recently, gravitational lensing in the strong gravity limit has been considered [16–22].

In the simplest case of a point-like gravitational lens (the Schwarzschild lens), the angular distances between images are on the order of the Einstein–Chwolson diameter $2\theta_0$, which is proportional to the square root of the lens mass (for fixed values of other parameters). At cosmological distances between objects and the typical mass $10^{12}M_\odot$ of the lensing galaxy, the angular distance between images is on the order of a few arcseconds; this is the standard gravitational macrolensing regime. For stellar-mass ($\sim M_\odot$) gravitational lenses at cosmological distances between the source, lens, and the image, the characteristic distance between the images is on the order of 10^{-6} arcseconds; this is the gravitational microlensing regime. If the mass of the gravitational lens is around the mass of Earth ($10^{-6}M_\odot$), the characteristic angular separation between the images is about 10^{-9} arcseconds (the gravitational nanolensing regime) (Table 1) (see Refs [12, 23, 24]). In fact, 10^{-9} arcseconds is a very small angle: for example, it corresponds to a coin 2.5 cm in diameter seen from a distance of 4.5×10^9 km (or about 30 AU, which is approximately the distance from the Sun to Neptune).

Table 1. Gravitational lensing regimes [12].

Regime	Deflection angle, arc s	Mass, $m/M_\odot$	Lens
Kilolensing	10^3	10^{18}	Supercluster
Macrolensing	10^0	10^{12}	Galaxy
Millilensing	10^{-3}	10^6	Black hole
Microlensing	10^{-6}	10^0	Star
Nanolensing	10^{-9}	10^{-6}	Planet (Earth-like)
Picolensing	10^{-12}	10^{-12}	?
Femtolensing	10^{-15}	10^{-18}	Comet

At present, micro- and nanoarcsecond angular resolutions are unreachable; however, the photometrical signatures of gravitational micro- and nanolensing can be obtained from the monitoring of background sources, as was proposed in Ref. [25]. Nevertheless, there are projects aimed at reaching an angular resolution of a few microarcseconds (in different spectral ranges), such as the NASA's Space Interferometry Mission (SIM) project, the ESA's Global Astrometric Interferometer for Astrophysics (GAIA) mission [26], the NASA's MicroArcsecond X-ray Imaging Mission (MAXIM) [27, 28] [2], and the Russian Radioastron mission. The nanosecond angular resolution in the millimeter wave band is planned to be achieved in the Millimetron space mission [3].

If the gravitational lens is a solar-mass ($M = M_\odot$) star in our Galaxy at a distance of 1 kpc, then $\theta_0 \approx 2'' \times 10^{-3}$. If the lens is an Earth-like ($M = 10^{-6}M_\odot$) planet located at the same distance from the observer, $\theta_0 \approx (2 \times 10^{-6})''$.

According to the terminology introduced above, if the lens mass is $M \sim M_\oplus$ ($M \sim 10^{-6}M_\odot$), the regime is called microlensing (nanolensing), irrespective of the characteristic distances. For example, one can talk of nanolensing when searching for planets by their contribution to the gravitational lensing.

The phenomenon of gravitational lensing can lead to the appearance of multiple images [1, 11]. For a point-like lens (the Schwarzschild lens), two images or a ring appear. The total solid angle of two images is larger than the solid angle of the source. The ratio of the sum of solid angles of both images to that of the source, which is called the amplification coefficient A of a gravitational lens, is just the result of gravitational focusing.

2. Gravitational microlensing

Gravitational microlensing has been intensively discussed in the literature [2, 15, 29–37]. If the source S lies on the Einstein–Chwolson cone, the amplification coefficient is $A = 1.34$. The corresponding characteristic time T_0 of microlensing is usually determined as the half-time it takes

[1] Chwolson [8] described the arising of ring-like images, and Einstein presented the basic equations for the gravitational focusing in the case of a point-like gravitational lens [9], now referred to in the literature as the Schwarzschild lens. It was realized later that Einstein had considered the phenomenon of gravitational focusing in unpublished notes [10] in 1912.

[2] Projects SIM and MAXIM will not likely be realized.

[3] See http://www.asc.rssi.ru.

for the lens to cross the Einstein–Chwolson cone:

$$T_0 = 3.5 \text{ months} \sqrt{\frac{M}{M_\odot}\frac{D_\mathrm{d}}{10 \text{ kpc}}}\,\frac{300 \text{ km s}^{-1}}{V_\perp},$$

where $V_\perp$ is the transverse velocity component of the lens. For $V_\perp \sim 300$ km s^{-1} (which is the characteristic velocity of stars in the Galaxy), the characteristic crossing time of the Einstein–Chwolson cone is about 3.5 months. Thus, the light curve of a background star changes on this time scale.

Some characteristic values of the parameters describing gravitational microlensing are as follows. For a distance between the lens and the Sun of about 10 kpc, the characteristic Einstein–Chwolson cone angle is about $0.001''$, which corresponds to linear distances of about 10 AU. Clearly, it is difficult to resolve such a small angular distance between the images by ground-based telescopes, at least in the optical range.

Einstein noted in due time that the phenomenon of gravitational lensing is difficult to discover in nature if the gravitational lens is a star, since the angle between the images is very small [4] [9]. Nonetheless, in the last few years the possibility of measuring the Einstein–Chwolson diameter $2\theta_0$ by resolving multiple images produced in microlensing has been discussed. In order to resolve multiple images, it was proposed to use an optical interferometer, for example, the VLTI (Very Large Telescope Interferometer) [38]. Moreover, in the astrometric space mission GAIA [5] to be launched in the near future, an angular resolution on the order of 10 microarcseconds can be achieved. In principle, this would allow one to resolve multiple images of sources arising due to microlensing. Astrometric microlensing in future astrometric missions was considered in papers [41, 42].

The phenomenon of microlensing in distant gravitationally lensed quasars was analyzed in paper [43], which was published shortly after the discovery of the first gravitational lensing system [44]. Due to a high optical depth (probability), this phenomenon was first disclosed in paper [45]. Later on, signatures of microlensing in different spectral ranges were found in various gravitational lens systems [46, 47], in particular, in SBS $1520+530$ in the optical spectrum, from observations carried out with the RTT-150 telescope [48]. The optical depth for microlensing of distant quasars was discussed in papers [49–52]. The influence of microlensing on light curves in different spectral ranges was analyzed in papers [53, 54]. The modeling of light curves (including X-ray light curves) was carried out after the discovery of X-ray microlensing for some gravitational lens systems [55–58] with the NASA's Chandra X-ray Observatory. Its telescope has an angular resolution of approximately 0.5 arcseconds, which enables, in principle, individual macro images in gravitational lens systems to be resolved.

The gravitational microlensing of a star by another star produces a symmetric and achromatic light curve, which is the main signature of the phenomenon. This statement holds true if the lens is spherically symmetric and the source is point-like. However, if the source is not point-like and the color is distributed across the stellar disk and (or) the gravitational field of the lens is not exactly spherically symmetric, then the light curve can be asymmetric and (or) chromatic [1].

The searches for microlensing events are closely related to the question of dark matter (DM). It has been known for a long time that only a small part of gravitating matter is visible [59, 60]. Presently, the matter density (in units of the critical density) is known to be $\Omega_\mathrm{m} \approx 0.3$ (including the baryonic matter density $\Omega_\mathrm{b} \approx 0.05-0.04$; however, the luminous matter density is $\Omega_\mathrm{lum} \leqslant 0.005$), and the density corresponding to the Λ-term is on the order of $\Omega_\Lambda = 0.7$ [61–64]. Thus, only a small part of the total matter density in the Universe is in the form of the baryonic matter density (to say nothing of the luminous matter). It is assumed often that galactic halos are quite 'natural' regions in which both baryonic and nonbaryonic dark matter can reside. If DM formed objects with masses in the range of $(10^{-5}-10)\,M_\odot$, microlensing could help detect them. Clearly, using microlensing, it is possible to discover dim low-mass stars and massive planets. Therefore, prior to the beginning of intensive microlensing observations in our and nearby galaxies, there was hope to shed light on the nature of dark matter in the halo of our Galaxy.

As noted above, the possibility of discovering microlensing phenomenon was discussed in paper [25]. Systematic searches for microlensing events using the characteristic features of the light curves of individual stars started after B Paczynski's discussion of the possibility of detecting compact dark objects of planetary or stellar masses in the Galactic halo by monitoring several million stars in the Large Magellanic Cloud (LMC) [65]. At the beginning of the 1990s, new calculation facilities and a huge amount of observational data appeared, which helped in relatively rapidly realizing Paczynski's ideas (the situation was significantly different when Byalko's paper [25] was published). It was proposed that such objects be referred to as 'machos' (after Massive Astrophysical Compact Halo Objects) [66]. What is more, MACHO is the name of the American–Australian–British collaboration which monitored stars in the LMC and the galactic bulge using the 1.3-meter telescope at the Mount Stromlo Observatory on Mount Stromlo in Australia. [6] To search for microlensing events, several million stars were monitored in the direction of two sky targets: (a) stars in the LMC and the Small Magellanic Cloud (SMC), since the LMC and SMC are nearby galaxies in the direction outside of the galactic plane, passing through the galactic halo, and (b) stars in the Galactic bulge, which allows one to estimate the distribution of microlenses in the direction close to the Galactic plane. The first microlensing events were reported in the direction toward the LMC by the MACHO collaboration [67] and by the EROS (Expérience pour la Recherche d'Objets Sombres) [7] French collaboration [69].

The first discovery of microlensing events towards the Galactic bulge was reported by the American–Polish OGLE (Optical Gravitational Lensing Experiment) collaboration, which employs the 1.3-meter telescope of the Las Campanas Observatory, Chile. In 2001, the third phase of the OGLE-III experiment started; in this experiment, 200 mln stars have been observed every 1–3 nights. During several recent years, the OGLE-III collaboration has discovered several hundred microlensing events each year [70, 71]. The OGLE-III phase was completed [8] in May 2009. The Early Warning System (EWS) helped to discover many microlensing events (Table 2).

[4] Nevertheless, microlensing can be discovered from observations of the variable light curves of background stars, as was proposed by Byalko [25].
[5] http://astro.setec.esa.nl/gaia, see also [26, 39, 40].
[6] The MACHO project was completed at the end of 1999.
[7] The EROS project was completed in 2003 [68].
[8] http://www.astrouw.edu.pl/ogle/ogle3/ews/ews.html.

Table 2. Microlensing events discovered in the OGLE-III experiment.

Year of observations	Number of events
2002	around 350
2003	around 450
2004	around 600
2005	around 550
2006	around 600
2007	around 600
2008	around 650

To search for microlensing events, astronomers in Japan and New Zealand formed the MOA (Microlensing Observations in Astrophysics) collaboration [9] [72].

To study the distribution of machos in a direction other than toward the LMC or SMC, the Andromeda Nebula (M31 galaxy) located at a distance of 778 kpc from the Sun can be used. This is a nearby galaxy in Earth's northern hemisphere [73–76]. In the 1990s, two collaborations, AGAPE (Andromeda Gravitational Amplification Pixel Experiment, Pic du Midi Observatory, France) [10] and VATT (Vatican Advanced Technology Telescope), started the monitoring of pixels, and not of individual stars [68, 80], since during observations of the Andromeda galaxy, many stars fall inside one pixel. At the present time, several dozen pixel lensing events have been reported [81, 82]. Monte Carlo simulations are necessary to theoretically interpret these observations [83–86].

As early as 15 years ago, it was clear that the microlensing phenomenon had really been discovered [30]. Nevertheless, it is difficult to precisely determine how many truly microlensing events were identified, since new types of stellar variability can have a similar observational appearance. [11] The most important results of the microlensing observations and their theoretical interpretation can be summarized as follows.

The observed light curves, which are related to microlensing candidate events, can be interpreted well by sufficiently simple theoretical models; however, this interpretation is sometimes questionable. For example, even for the MACHO No. 1 event different fits by a single microlens were reported, but significant deviations between the theoretical curve and experimental data near the light curve maximum were seen. Still, a binary microlens model yields a much better fit which fully agrees with observations [87, 88]. The fit by a non-compact microlens model was also proposed [89–97].

For the EROS BLG-2000-5 event, the PLANET (Probing Lensing Anomalies NETwork) collaboration determined the component masses of a binary microlens, $0.35\,M_\odot$ and $0.262\,M_\odot$, and the distance to the lens, 2.6 kpc from the Sun [98].

Some extended microlensing events were connected with stellar-mass black holes [99]. For example, the initial mass estimates for the MACHO-96-BLG-5 and MACHO-96-BLG-6 events were reported to be $M/M_\odot = 6^{+10}_{-3}$ and $M/M_\odot = 6^{+7}_{-3}$, respectively, i.e., the mass exceeded the Oppenheimer–Volkoff limit, suggesting microlensing by black holes. Later estimates showed that the MACHO-99-BLG-22, MACHO-96-BLG-5, and MACHO-96-BLG-6 events can be associated with black holes with a probability falling down from 78% to 37%, and to 2%, respectively [100].

The optical depth in the direction of the Galactic bulge (on the order of 3×10^{-6}) turned out to be somewhat larger than the initial estimates [101], which additionally supports the existence of a bar-like structure.

The MACHO collaboration analyzed the data obtained during 5.7 years of photometry of 11.9 mln stars in the LMC and discovered 13–17 microlensing event candidates [102] (the number of candidates depends on the selection rule applied). The optical depth toward the LMC obtained from the observations, $\tau(2 < \hat{t} < 400\,\text{days}) = 1.2^{+0.4}_{-0.3} \times 10^{-7}$ (here $\hat{t}$ is the microlensing event duration), turned out to be smaller than a theoretical estimate based on the assumption that the halo dark mass falls within macho-like objects. Based on the MACHO collaboration observations, the most likely fraction of machos in the halo mass is $f = 0.2$. The following probability estimates were also reported: $P(0.08 < f < 0.5) = 0.95$, and $P(f = 1) < 0.05$. The most likely estimate of the mass of a macho is $M = (0.15-0.9)\,M_\odot$, and the halo mass within the sphere of radius 50 kpc must be about $9^{+4}_{-3} \times 10^{10}\,M_\odot$.

The EROS collaboration reported the probability estimate $P(M \in [10^{-7}, 1]\,M_\odot,\ f > 0.4) < 0.05$ [103, 104] and the estimate of the optical depth toward the LMC, $\tau < 0.36 \times 10^{-7}$ (at a 95% C.L.), which means that the macho mass fraction in the total halo mass is no higher than 7% [105].

On the other hand, the OGLE collaboration estimated the macho mass fraction in the halo mass as $(8 \pm 6)\%$ [106]. Essentially, this means the lack of macho detection if their abundance in the galactic halo is at the level of 19% for $M = 0.4\,M_\odot$, and 10% for the mass range $(0.01–0.2)\,M_\odot$ [106]. However, these conclusions are based on an assumption about the form of the mass and space distributions of microlenses, which are poorly known. In principle, the gravitational microlensing studies can be used to improve the parameters of these distributions, provided that several thousand microlensing events are available.

Thus, the following general conclusion can be made. A very important physical phenomenon, gravitational microlensing, was discovered, but some of its quantitative characteristics must be improved. Therefore, the question of the nature of about 80% (or even 93%, according to the EROS collaboration) of the galactic halo dark matter persists (before the microlensing observations, there was a hope to significantly advance in solving the dark matter question). So, the situation is quite adequately reflected by the title of Kerins's report [107], "Machos and clouds of uncertainty." This means that there is a wide field for future research, including pixel lensing and microlensing of gravitationally lensed systems, with the most interesting and important being searches for exoplanets using microlensing.

3. Methods of searching for exoplanets

Nearly 20 years ago, Mao and Paczynski [108] estimated the probability of finding exoplanets using the microlensing phenomenon, and noted that this probability is highest in the direction toward the Galactic bulge. In spite of the fact that the first exoplanet was discovered around the millisecond pulsar PSR 1257 + 12 [109], this prediction by Mao and

[9] http://www.roe.ac.uk/%7Eliab/alert/alert.html.

[10] The POINT-AGAPE (POINT — after Pixel-lensing Observation with the Isaac Newton Telescope (INT)) collaboration started observations in 1999 using INT with a 2.5-m mirror [77, 78]; the robotic telescope MIT Angstrom Project was also proposed [79].

[11] Some events, first reported to be microlensing candidates by the EROS-1, EROS-2, MACHO-2, and MACHO-3 collaborations, were later interpreted in terms of stellar variability [30].

Paczynski proved to be essentially correct, and presently microlensing is recognized as an effective method of searching for exoplanets.

The most effective method of discovering exoplanets is based on radial velocity measurements using the HARPS (High Accuracy Radial velocity Planet Searcher) spectrograph. This spectrograph is mounted on the 3.6-m telescope of the European Southern Observatory at La Silla (Chile). The typical measurement error is ~ 1 m s^{-1}, more precisely, varying within the range of 0.7–2 m s^{-1}, depending on the observational conditions [110]. Radial velocity estimates are listed in Table 1 of review [111]. Using this method, more than 300 exoplanets have been found to date.

About 100 exoplanets have been discovered taking advantage of the transit method. Some transits (observed both by ground-based and space telescopes [12]) are described in paper [112] (see also Table 2 in review [111]). The launch of the Kepler space telescope increases significantly the efficiency of the transit method for discovering exoplanets. Let us recall that the Kepler telescope has a mirror diameter which is more than three times larger than that of the COROT (COnvection ROtation and planetary Transits) space telescope, and the field of view more than 100 times larger than that of COROT. The COROT group discovered interesting planetary systems, such as the COROT-7b planet with a radius of about two Earth radii [113]. The follow-up observations of this system with the HARPS spectrograph detected two exoplanets with near-Earth masses: $(4.8\pm 0.8)\,M_\oplus$ (COROT-7b), and $(8.4 \pm 0.9)\,M_\oplus$ (COROT-7c) [114].

According to the database collected by Jean Schneider (CNRS–LUTH, Paris Observatory),[13] by now more than 500 exoplanets and about 400 exoplanet candidates have been discovered; nevertheless, there are no reliable criteria to distinguish between them. Several planetary systems have been discovered by pulsar timing.

One exoplanet was found by astrometric measurements (see, for example, the Jet Propulsion Laboratory press release of May 28, 2009,[14] and there is hope that new planetary systems will be discovered by this method in the forthcoming space missions, such as the James Webb Space Telescope (JWST) and GAIA.

It is important that there is a possibility of using different exoplanet search methods to be certain that the assertion about the existence of planets made with the aid of a single search method is valid. The radial velocity method and transits and (or) astrometric measurements can be complementary to each other (for example, the radial velocities of Gliese 876b were measured and the exoplanet was observed by the HST). For more details see Refs [111, 115–118].

4. Searches for exoplanets using gravitational microlensing

As the presence of a planet near the star-lens breaks the symmetry of the lens system, fold caustics [11, 119, 120] arise, resulting in the appearance of the characteristic deviations in the light curve of the star-lens from the case without a planet. These features are used to discover exoplanets by gravitational microlensing. Thus, it is necessary first to find a microlensing event, and then to measure the characteristic deviation in the observed light curve. It should be noted that monitoring of a large number of stars is needed to detect microlensing events, while observations of the light curves of the background stars with microlensing signatures are required for discovering exoplanets. The latter can be done using relatively small telescopes with a small field of vision. In this case, it is very important to have an early alert monitoring system for microlensing event candidates, similar to that organized by the OGLE collaboration.

Table 3. Exoplanets discovered by the microlensing [123–126].

Mass of star	Mass of planet	Principal semiaxis, AU
$0.63^{+0.07}_{-0.09}\,M_\odot$	$830^{+250}_{-190}\,M_\oplus$	$4.3^{+2.5}_{-0.8}$
$(0.46 \pm 0.04)\,M_\odot$	$(1100 \pm 100)\,M_\oplus$	4.4 ± 1.8
$0.22^{+0.21}_{-0.11}\,M_\odot$	$5.5^{+5.5}_{-2.7}\,M_\oplus$	$2.6^{+1.5}_{-0.6}$
$0.49^{+0.14}_{-0.18}\,M_\odot$	$13^{+4.0}_{-5.0}\,M_\oplus$	$3.2^{+1.5}_{-1.0}$
$(0.50 \pm 0.04)\,M_\odot$	$(226 \pm 25)\,M_\oplus$	2.3 ± 0.2
$(0.50 \pm 0.04)\,M_\odot$	$(86 \pm 10)\,M_\oplus$	4.6 ± 0.5
$0.060^{+0.028}_{-0.021}\,M_\odot$	$3.3^{+4.9}_{-1.6}\,M_\oplus$	$0.62^{+0.22}_{-0.16}$
$0.30^{+0.19}_{-0.12}\,M_\odot$	$260.54^{+165.22}_{-104.85}\,M_\oplus$	$\begin{cases} 0.72^{+0.38}_{-0.16} \\ \text{or } 6.5^{+3.2}_{-1.2} \end{cases}$

As noted in Section 3, Mao and Paczynski [108] stressed that the probability of discovering exoplanets using microlensing is sufficiently high (see also papers [121, 122]). These conclusions are supported by available observations.

Exoplanets discovered by microlensing observations in the direction of the Galactic bulge are listed in Table 3 [123–127]. For the planetary system in the last row of this table, two possible distance intervals between the planet and star-lens are given [123, 128]. Discoveries of exoplanets were discussed in papers [71, 123, 124, 126, 129–132]. It should be noted that the first exoplanet was discovered by the MOA-I collaboration, which used a small 0.6-m telescope [123, 129]. This microlensing event was discovered by the OGLE collaboration, but the MOA-I group had a CCD (charge-coupling device) with a larger field of view and made five exposures per field of view. This fact clearly shows that important results can be obtained by even modest observational facilities used in the right way.

Eight exoplanets were discovered by microlensing, including three Earth-group exoplanets with masses $10M_\oplus$ (which are also called super-Earth exoplanets). Table 3 illustrates that this technique is very effective in detecting Earth-group exoplanets located at a distance of 1 AU from the star-lens.

The detection of an exoplanet with the mass of about $5.5\,M_\oplus$ [133] is one of the most important discoveries. It was the lightest exoplanet in 2006. [15] Essentially, this means that Earth-group planets with a solid surface have a sufficiently wide spread in the Universe [130, 134, 135].

Pixel microlensing in the direction of the Andromeda galaxy (M31) can be an effective means of discovering exoplanets in other galaxies [136–141]. In this case, the emission from several thousand stars falls within one pixel,

[12] Recently, the Kepler space mission reported the discovery of about 1000 exoplanets.

[13] http://www.exoplanet.eu.

[14] http://www.jpl.nasa.gov/news/news.cfm?release = 2009-090.

[15] Later on, the discovery of a light exoplanet with $m_p \sin i = 1.94\,M_\oplus$ at a distance of order 0.03 AU in the Gliese 581 b system (GJ 581 b), which has several exoplanets, was reported [110].

and then only the lensing of giant stars can result in detectable radiation flux variations in one pixel. Giant stars can have radii on the order of 1 AU (the distance from Earth to the Sun); therefore, the probability estimates of the potentially detectable deviation of the light curve of a star-lens with an exoplanet from the case without exoplanets should be made using Monte Carlo simulations of the pixel lensing [138, 139].

Since the discovery of an exoplanet using pixel lensing is naturally divided into two stages (namely, searches for pixel lensing events and detection of the exoplanet signatures in these events), an early alert online system seems to be required for research groups involved in the Andromeda galaxy monitoring, as was done by the OGLE collaboration for microlensing searches in the Galactic bulge. This system would allow even small telescopes with a narrow field of view to be used in monitoring the pixel lensing candidates and, possibly, to discover deviations from the light curve, signaling the presence of an exoplanet in the lens system.

The PA-N2-99 event observed by the POINT-AGAPE collaboration [142] showed an anomaly which is most likely due to the presence of a panet system in the lens [138–140]. This suggests that the first extragalactic exoplanet has been found. For example, in Wikipedia's article about the Andromeda galaxy, one can read that an exoplanet was discovered around a star in this galaxy, with a reference to paper [138]. As mentioned above, stellar sources for pixel lensing are red giants (we recall that the lensing of only giants leads to detectable effects, since there are many thousands of stars in one pixel). Therefore, their size is comparable to the Einstein–Chwolson radius and the size of caustics, and the finite size of the sources should be taken into account, as in searches for quasar microlensing events [53, 143]. It is well known [144–152] that the amplification of a point-like source is different from the analogous parameter of a finite-size source. If the source diameter is small, the probability of discovering the signatures of a binary lens (or a planet near the star) is proportional to the size of the region near the caustic. Nevertheless, giant stars considered as background sources have larger angular sizes, so the probability that some part of the source is close to the caustic increases (see papers [138–140] for more detail).

5. Conclusions

Several dozen super-Earth exoplanets [16] with masses in the range (1–10) $M_\oplus$ have been discovered by different means [110, 124, 130, 157–164]. It is easy to see that the fraction of Earth-mass exoplanets detected by gravitational microlensing is rather high in comparison with exoplanets found by other methods. Searches for low-mass exoplanets are related to searches for life in the Universe. The locations of exoplanets near the habitation zone [165–167] are being studied in detail using different methods, including the dynamical analysis of multiplanet systems [168–177]. Clearly, Earth-mass planetary systems with distances of about 1 AU between the stars and such planets are the most intriguing from this point of view. Gravitational microlensing is a very effective method of searching for such exoplanets. In this context, the MPF (Microlensing Planet Finder) American project can be much more effective than other dedicated space missions for exoplanet searches (see Fig. 2 in paper [125], and Fig. 1.9 in paper [123]).

[16] Their physical properties are a field of intensive studies [153–156].

For distant planetary systems discovered by microlensing (or pixel lensing), using other additional methods is rather difficult (at least at present), since these methods are not sensitive enough for such systems. Nevertheless, direct observations of a planet, for example, by a space telescope [178], can be useful in reducing uncertainty in the estimates of the parameters of the planetary system. An interesting possibility for directly observing Earth-like exoplanets can be realized using a space telescope and a stellar screen that significantly decreases the emission flux from the star possessing an exoplanet. Such a possibility is being discussed in the New Worlds Observer project [179–181]. It is assumed that the screen and telescope will be located in the vicinity of the Lagrangian L_2 point. The telescope has a diameter of about 4 m, the size of the screen is of order 50 m, and the distance between the screen and the telescope is on the order of 80,000 km. Such an approach was earlier discussed in the literature; however, the technical feasibility of detecting low-mass exoplanets by a screen several dozen meters in diameter was noticed quite recently [182]. Thus, at the present time the principal technology for direct detection of low-mass exoplanets is available.

Acknowledgments. The author wishes to express his appreciation to S Calchi Novati, W Cash, F de Paolis, Ph Jetzer, G Ingrosso, P Jovanović, A Nucita, L Č Popović, M V Sazhin, and A M Cherepashchuk for valuable discussions of different aspects of the gravitational lensing and searches for exoplanets.

References

1. Zakharov A F *Gravitatsionnye Linzy i Mikrolinzy* (Gravitational Lenses and Microlenses) (Moscow:Yanus-K, 1997)
2. Zakharov A F, Sazhin M V *Usp. Fiz. Nauk* **168** 1041 (1998) [*Phys. Usp.* **41** 945 (1998)]
3. Newton I *Opticks*: *or a Treatise of the Reflexions, Refractions, Inflexions and Colours of Light* (London: Printed for S Smith, and B Walford, 1704)
4. Soldner J G *Berliner Astron. Jahrbuch* 161 (1804)
5. Einstein A *Ann. Physik* **49** 769 (1916) [Translated into Russian: *Sobranie Sochinenii* (Collected Works) Vol. 1 (Moscow: Nauka, 1965) p. 452]
6. Dyson F W, Eddington A S, Davidson C *Philos. Trans. R. Soc. London A* **220** 291 (1920)
7. Eisenstaedt J *The Curious History of Relativity* (Princeton, N.J.: Princeton Univ. Press, 2006)
8. Chwolson O *Astron. Nachrich.* **221** 329 (1924)
9. Einstein A *Science* **84** 506 (1936)
10. Renn J, Sauer T, Stachel J *Science* **275** 184 (1997)
11. Schneider P, Ehlers J, Falco E E *Gravitational Lenses* (Berlin: Springer-Verlag, 1992)
12. Wambsganss J, in *Gravitational Lenses in the Universe*: *Proc. of the 31st Liege Intern. Astrophysical Colloquium* (*LIAC 93*) (Eds J Surdej et al.) (Liege: Univ. de Liege, Institut d'Astrophysique, 1993) p. 369
13. Refsdal S, Surdej J *Rep. Prog. Phys.* **56** 117 (1994)
14. Claeskens J-F, Surdej J *Astron. Astrophys. Rev.* **10** 263 (2002)
15. Mollerach S, Roulet E *Gravitational Lensing and Microlensing* (Singapore: World Scientific, 2002)
16. Frittelli S, Kling T P, Newman E T *Phys. Rev. D* **61** 064021 (2000)
17. Bozza V et al. *Gen. Relat. Grav.* **33** 1535 (2001)
18. Virbhadra K S, Ellis G F R *Phys. Rev. D* **65** 103004 (2002)
19. Zakharov A F et al. *New Astron.* **10** 479 (2005)
20. Zakharov A F et al. *Astron. Astrophys.* **442** 795 (2005)
21. Virbhadra K S, Keeton C R *Phys. Rev. D* **77** 124014 (2008)
22. Virbhadra K S *Phys. Rev. D* **79** 083004 (2009)
23. Zakharov A F *New Astron. Rev.* **53** 202 (2009)
24. Zackrisson E, Riehm T, arXiv:0905.4075
25. Byalko A V *Astron. Zh.* **46** 998 (1969) [*Sov. Astron.* **13** 784 (1970)]

26. Lindegren L, Perryman M A C *Astron. Astrophys. Suppl.* **116** 579 (1996)
27. Cash W et al. *Nature* **407** 160 (2000)
28. White N *Nature* **407** 146 (2000)
29. Wu X-P *Astrophys. J.* **435** 66 (1994)
30. Paczyński B *Annu. Rev. Astron. Astrophys.* **34** 419 (1996)
31. Roulet E, Mollerach S *Phys. Rep.* **279** 67 (1997)
32. Mao S *AIP Conf. Proc.* **237** 215 (2001); astro-ph/9909302
33. Jetzer Ph *Naturwissenschaften* **86** 201 (1999)
34. Zakharov A F *Publ. Astron. Observ. Belgrade* (75) 27 (2003)
35. Zakharov A F, in *Particle Physics in Laboratory, Space and Universe*: *Proc. of the 11th Lomonosov Conf. on Elementary Particle Physics, August 21–27, 2003, Moscow, Russia* (Ed. A I Studenikin) (Singapore: World Scientific, 2005) p. 106
36. Mao S, arXiv:0811.0441
37. Zakharov A F *Phys. Part. Nucl.* **39** 1176 (2008)
38. Delplancke F, Górski K M, Richichi A *Astron. Astrophys.* **375** 701 (2001)
39. Perryman M A C et al. *Astron. Astrophys.* **369** 339 (2001)
40. Perryman M, de Bruijne J, Lammers U *Exp. Astron.* **22** 143 (2008)
41. Zakharov A F *Astron. Zh.* **83** 99 (2006) [*Astron. Rep.* **50** 79 (2006)]
42. Zakharov A F *Int. J. Mod. Phys. D* **17** 1055 (2008)
43. Gott J R (III) *Astrophys. J.* **243** 140 (1981)
44. Walsh D, Carswell R F, Weymann R J *Nature* **279** 381 (1979)
45. Irwin M J et al. *Astron. J.* **98** 1989 (1989)
46. Sluse D et al. *Astron. Astrophys.* **468** 885 (2007)
47. Sluse D et al., arXiv:0809.2983
48. Khamitov I M et al. *Pis'ma Astron. Zh.* **32** 570 (2006) [*Astron. Lett.* **32** 514 (2006)]
49. Canizares C R *Astrophys. J.* **263** 508 (1982)
50. Zakharov A F, Popović L Č, Jovanović P *Astron. Astrophys.* **420** 881 (2004)
51. Zakharov A F, Popović L Č, Jovanović P, in *Gravitational Lensing Impact on Cosmology*: *Proc. of the 225 IAU Symp.* (Eds Y Mellier, G Meylan) (Cambridge: Cambridge Univ. Press, 2005) p. 363
52. Zakharov A F, Popović L Č, Jovanović P, in *Exploring the Universe*: *Proc. of the XXXIXth Rencontres de Moriond Workshop* (Eds Y Giraud-Heraud, J Trân Thanh Vân, J Dumarchez) (Hanoi: GIOI Publ., 2005) p. 41
53. Popović L Č et al. *Astrophys. J.* **637** 620 (2006)
54. Jovanović P et al. *Mon. Not. R. Astron. Soc.* **386** 397 (2008)
55. Chartas G et al. *Astrophys. J.* **568** 509 (2002)
56. Chartas G et al. *Astrophys. J.* **606** 78 (2004)
57. Dai X et al. *Astrophys. J.* **589** 100 (2003)
58. Dai X et al. *Astrophys. J.* **605** 45 (2004)
59. Oort J *Bull. Astron. Inst. Netherlands* **6** 249 (1932)
60. Zwicky F *Helv. Phys. Acta* **6** 110 (1933)
61. Astier P et al. *Astron. Astrophys.* **447** 31 (2006)
62. Komatsu E et al. *Astrophys. J. Suppl.* **180** 330 (2009)
63. Zakharov A F et al. *Space Sci. Rev.* **148** 301 (2009)
64. Zakharov A F et al. *Yad. Fiz.* **73** 1921 (2010) [*Phys. Atom. Nucl.* **73** 1870 (2010)]
65. Paczynski B *Astrophys. J.* **304** 1 (1986)
66. Griest K *Astrophys. J.* **366** 412 (1991)
67. Alcock C et al. *Nature* **365** 621 (1993)
68. Moniez M, in *Cosmological Physics with Gravitational Lensing*: *Proc. of the XXXVth Rencontres de Moriond, Les Arcs, France, March 11–18, 2000* (Eds J Trân Thanh Vân, Y Mellier, M Moniez) (Les Ulis: EDP Sci., 2001) p. 3
69. Aubourg E et al. *Nature* **365** 623 (1993)
70. Udalski A et al. *Acta Astron.* **53** 291 (2003)
71. Udalski A et al. *Astrophys. J.* **628** L109 (2005)
72. Bond I A et al. *Mon. Not. R. Astron. Soc.* **327** 868 (2001)
73. Crotts A P S *Astrophys. J.* **399** L43 (1992)
74. Baillon P et al. *Astron. Astrophys.* **277** 1 (1993)
75. Ansari R et al., astro-ph/9602015
76. Ansari R et al. *Astron. Astrophys.* **324** 843 (1997)
77. Kerins E et al. *Mon. Not. R. Astron. Soc.* **323** 13 (2001)
78. Belokurov V et al. *Mon. Not. R. Astron. Soc.* **357** 17 (2005)
79. Kerins E et al. *Mon. Not. R. Astron. Soc.* **365** 1099 (2006)
80. Le Du Y, in *Cosmological Physics with Gravitational Lensing*: *Proc. of the XXXVth Rencontres de Moriond, Les Arcs, France, March 11–18, 2000* (Eds J Trân Thanh Vân, Y Mellier, M Moniez) (Les Ulis: EDP Sci., 2001) p. 65
81. Calchi Novati S et al. *Astron. Astrophys.* **443** 911 (2005)
82. Calchi Novati S et al. *Astrophys. J.* **695** 442 (2009)
83. De Paolis F et al. *Astron. Astrophys.* **432** 501 (2005)
84. Ingrosso G et al. *Astron. Astrophys.* **445** 375 (2006)
85. Ingrosso G et al. *Astron. Astrophys.* **462** 895 (2007)
86. Riffeser A, Seitz S, Bender R *Astrophys. J.* **684** 1093 (2008)
87. Dominik M, Hirshfeld A C *Astron. Astrophys.* **289** L31 (1994)
88. Dominik M, Hirshfeld A C *Astron. Astrophys.* **313** 841 (1996)
89. Gurevich A V, Zybin K P, Sirota V A *Phys. Lett. A* **214** 232 (1996)
90. Gurevich A V, Zybin K P, Sirota V A *Usp. Fiz. Nauk* **167** 913 (1997) [*Phys. Usp.* **40** 869 (1997)]
91. Zakharov A F, Sazhin M V *Pis'ma Zh. Eksp. Teor. Fiz.* **63** 894 (1996) [*JETP Lett.* **63** 937 (1996)]
92. Zakharov A F, Sazhin M V *Zh. Eksp. Teor. Fiz.* **110** 1921 (1996) [*JETP* **83** 1057 (1996)]
93. Zakharov A F *Phys. Lett. A* **250** 67 (1998)
94. Zakharov A F *Astron. Zh.* **76** 379 (1999) [*Astron. Rep.* **43** 325 (1999)]
95. Zakharov A F, in *Dark Matter in Astro- and Particle Physics*: *Proc. of the Intern. Conf. DARK 2000, Heidelberg, Germany, 10–14 July, 2000* (Ed. H V Klapdor-Kleingrothaus) (Berlin: Springer-Verlag, 2001) p. 364
96. Zakharov A F, in *Cosmological Physics with Gravitational Lensing*: *Proc. of the XXXVth Rencontres de Moriond, Les Arcs, France, March 11–18, 2000* (Eds J Trân Thanh Vân, Y Mellier, M Moniez) (Les Ulis: EDP Sci., 2001) p. 57
97. Zakharov A *Gen. Relat. Grav.* **42** 2301 (2010)
98. An J H et al. *Astrophys. J.* **572** 521 (2002)
99. Bennett D P et al. *Astrophys. J.* **579** 639 (2002)
100. Poindexter S et al. *Astrophys. J.* **633** 914 (2005)
101. Alcock C et al. *Astrophys. J.* **541** 734 (2000)
102. Alcock C et al. *Astrophys. J.* **542** 281 (2000)
103. Lasserre T et al. *Astron. Astrophys.* **355** L39 (2000)
104. Lasserre T, in *Dark Matter in Astro- and Particle Physics*: *Proc. of the Intern. Conf. DARK 2000, Heidelberg, Germany, 10–14 July, 2000* (Ed. H V Klapdor-Kleingrothaus) (Berlin: Springer-Verlag, 2001) p. 341
105. Tisserand P et al. *Astron. Astrophys.* **469** 387 (2007)
106. Wyrzykowski L et al. *Mon. Not. R. Astron. Soc.* **397** 1228 (2009); arXiv:0905.2044
107. Kerins E, in *Cosmological Physics with Gravitational Lensing*: *Proc. of the XXXVth Rencontres de Moriond, Les Arcs, France, March 11–18, 2000* (Eds J Trân Thanh Vân, Y Mellier, M Moniez) (Les Ulis: EDP Sci., 2001) p. 43
108. Mao S, Paczynski B *Astrophys. J. Lett.* **374** L37 (1991)
109. Wolszczan A, Frail D A *Nature* **355** 145 (1992)
110. Mayor M et al. *Astron. Astrophys.* **507** 487 (2009); arXiv:0906.2780
111. Perryman M et al. "Report by the ESA–ESO Working Group on Extra-Solar Planets", http://www.stecf.org/coordination/eso-esa/extrasolar/report.pdf; astro-ph/0506163
112. Konacki M et al. *Nature* **421** 507 (2003)
113. Léger A et al. *Astron. Astrophys.* **506** 287 (2009)
114. Queloz D et al. *Astron. Astrophys.* **506** 303 (2009)
115. Perryman M A C *Rep. Prog. Phys.* **63** 1209 (2000)
116. Udry S, Santos N C *Annu. Rev. Astron. Astrophys.* **45** 397 (2007)
117. Santos N C *New Astron. Rev.* **52** 154 (2008)
118. Johnson J A *Publ. Astron. Soc. Pacific* **121** 309 (2009)
119. Zakharov A F *Astron. Astrophys.* **293** 1 (1995)
120. Zakharov A F *Astrophys. Space Sci.* **252** 369 (1997)
121. Gould A, Loeb A *Astrophys. J.* **396** 104 (1992)
122. Bolatto A D, Falco E E *Astrophys. J.* **436** 112 (1994)
123. Bennett D P, in *Exoplanets* (Ed. J Mason) (Berlin: Springer, 2008) p. 47; arXiv:0902.1761
124. Bennett D P et al. *Astrophys. J.* **684** 663 (2008)
125. Bennett D P et al. "A census of exoplanets in orbits beyond 0.5 AU via space-based microlensing", White Paper for the Astro2010 Science Frontier Panel (2008); arXiv:0902.3000
126. Dong S et al. *Astrophys. J.* **698** 1826 (2009)
127. Zakharov A F et al. *Mem. Soc. Astron. Italiana Suppl.* **15** 114 (2010)
128. Dominik M *Astron. Astrophys.* **349** 108 (1999)
129. Bond I A et al. *Astrophys. J. Lett.* **606** L155 (2004)
130. Beaulieu J-P et al. *Nature* **439** 437 (2006)

131. Gould A et al. *Astrophys. J.* **644** L37 (2006)
132. Gaudi B S et al. *Science* **319** 927 (2008)
133. Abe F et al. *Science* **305** 1264 (2004)
134. Dominik M *Mon. Not. R. Astron. Soc.* **367** 669 (2006)
135. Dominik M, Horne K, Bode M F *Astron. Geophys.* **47** 3.25 (2006)
136. Chung S-J et al. *Astrophys. J.* **650** 432 (2006)
137. Kim D et al. *Astrophys. J.* **666** 236 (2007)
138. Ingrosso G et al. *Mon. Not. R. Astron. Soc.* **399** 219 (2009)
139. Ingrosso G et al. *Gen. Relat. Grav.* **43** 1047 (2011); arXiv:1001.4342
140. Ingrosso G et al., arXiv:1001.2105
141. Dominik M et al. *Astron. Nachrichten* **331** 671 (2010)
142. An J H et al. *Astrophys. J.* **601** 845 (2004)
143. Agol E, Krolik J *Astrophys. J.* **524** 49 (1999)
144. Witt H J, Mao S *Astrophys. J.* **430** 505 (1994)
145. Bogdanov M B, Cherepashchuk A M *Pis'ma Astron. Zh.* **21** 570 (1995) [*Astron. Lett.* **21** 505 (1995)]
146. Bogdanov M B, Cherepashchuk A M *Astron. Zh.* **72** 873 (1995) [*Astron. Rep.* **39** 779 (1995)]
147. Bogdanov M B, Cherepashchuk A M *Astron. Zh.* **77** 842 (2000) [*Astron. Rep.* **44** 745 (2000)]
148. Bogdanov M B, Cherepashchuk A M *Astron. Zh.* **79** 1102 (2002) [*Astron. Rep.* **46** 996 (2002)]
149. Gaudi B S, Gould A *Astrophys. J.* **513** 619 (1999)
150. Dominik M *Mon. Not. R. Astron. Soc.* **361** 300 (2005)
151. Heyrovský D *Astrophys. J.* **656** 483 (2007)
152. Pejcha O, Heyrovský D *Astrophys. J.* **690** 1772 (2009)
153. Valencia D, Sasselov D D, O'Connell R J *Astrophys J.* **665** 1413 (2007)
154. Selsis F et al. *Astron. Astrophys.* **476** 1373 (2007)
155. Sasselov D D *Nature* **451** 29 (2008)
156. Sasselov D D, Valencia D, O'Connell R J *Phys. Scripta* **T130** 014035 (2008)
157. Rivera E J et al. *Astrophys. J.* **634** 625 (2005)
158. Lovis C et al. *Nature* **441** 305 (2006)
159. Udry S et al. *Astron. Astrophys.* **469** L43 (2007)
160. Marcy G W et al. *Phys. Scripta* **T130** 014001 (2008)
161. Mayor M, Udry S *Phys. Scripta* **T130** 014010 (2008)
162. Mayor M et al. *Astron. Astrophys.* **493** 639 (2009)
163. Bouchy F et al. *Astron. Astrophys.* **496** 527 (2009)
164. Howard A W et al. *Astrophys. J.* **696** 75 (2009)
165. Kasting J F, Whitmire D P, Reynolds R T *Icarus* **101** 108 (1993)
166. Jones B W, Underwood D R, Sleep P N *Astrophys. J.* **622** 1091 (2005)
167. Lammer H et al. *Astron. Astrophys. Rev.* **17** 181 (2009)
168. Ji J et al. *Astrophys. J.* **585** L139 (2003)
169. Ji J et al. *Astrophys. J.* **631** 1191 (2005)
170. Ji J et al. *Astrophys. J.* **657** 1092 (2007)
171. Fischer D A et al. *Astrophys. J.* **675** 790 (2008)
172. Pilat-Lohinger E et al. *Astrophys. J.* **681** 1639 (2008)
173. Pilat-Lohinger E *Int. J. Astrobiol.* **8** 175 (2009)
174. Ji J-H et al. *Res. Astron. Astrophys.* **9** 703 (2009)
175. McNeil D S, Nelson R P *Mon. Not. R. Astron. Soc.* **401** 1691 (2010); arXiv:0910.5299
176. Wright J T, arXiv:0909.0957
177. Wright J T et al. *Astrophys. J.* **693** 1084 (2009)
178. Bennett D P et al. *Astrophys. J.* **647** L171 (2006)
179. Oakley P H H, Cash W *Astrophys. J.* **700** 1428 (2009)
180. Cash W (and the New Worlds Team) *EPJ Web Conf.* **16** 07004 (2011)
181. Cash W *Astrophys. J.* **738** 76 (2011); arXiv:1106.2127
182. Cash W *Nature* **442** 51 (2006)